Development of the human prostate

Gerald R. Cunha[1,*], **Chad M. Vezina**[2], **Dylan Isaacson**[1], **William A. Ricke**[3], **Barry G. Timms**[4], **Mei Cao**[1], **Omar Franco**[5], and **Lawrence S. Baskin**[1]

[1]Department of Urology, University of California, 400 Parnassus Avenue, San Francisco, CA 94143

[2]School of Veterinary Medicine, University of Wisconsin, Madison, Wisconsin 53706

[3]Department of Urology, University of Wisconsin, Madison, WI 53705

[4]Division of Basic Biomedical Sciences, Sanford School of Medicine, University of South Dakota, Vermillion, SD 57069

[5]Department of Surgery, North Shore University Health System, 1001 University Place, Evanston, IL 60201

Abstract

This paper provides a detailed compilation of human prostatic development that includes human fetal prostatic gross anatomy, histology, and ontogeny of selected epithelial and mesenchymal differentiation markers and signaling molecules throughout the stages of human prostatic development: (a) pre-bud urogenital sinus (UGS), (b) emergence of solid prostatic epithelial buds from urogenital sinus epithelium (UGE), (c) bud elongation and branching, (d) canalization of the solid epithelial cords, (e) differentiation of luminal and basal epithelial cells, and (f) secretory cytodifferentiation. Additionally, we describe the use of xenografts to assess the actions of androgens and estrogens on human fetal prostatic development. In this regard, we report a new model of de novo DHT-induction of prostatic development from xenografts of human fetal female urethras, which emphasizes the utility of the xenograft approach for investigation of initiation of human prostatic development. These studies raise the possibility of molecular mechanistic studies on human prostatic development through the use of tissue recombinants composed of mutant mouse UGM combined with human fetal prostatic epithelium. Our compilation of human prostatic developmental processes is likely to advance our understanding of the pathogenesis of benign prostatic hyperplasia and prostate cancer as the neoformation of ductal-acinar architecture during normal development is shared during the pathogenesis of benign prostatic hyperplasia and prostate cancer.

*Corresponding author, Department of Urology, University of California, 400 Parnassus Avenue, San Francisco, CA 94143, Gerald.cunha@ucsf.edu.

Introduction

The prostate arises from epithelial buds that emerge from the embryonic urogenital sinus (UGS). Prostatic development has been studied in many mammalian species. While species-specific details of prostatic development and anatomy have been noted, the developmental process is remarkably similar in all species examined. The most detailed description of prostatic development has been reported for the mouse and rat, while prostatic development in the human is especially incomplete and under-represented in the literature. Prostatic development can be subdivided into several stages: (a) pre-bud UGS, (b) emergence of solid prostatic epithelial buds from urogenital sinus epithelium (UGE), (c) bud elongation and branching, (d) canalization of the solid epithelial cords, (e) differentiation of luminal and basal epithelial cells, and (f) secretory cytodifferentiation (Table 1). In all species investigated, testosterone production by the fetal testes begins in the pre-bud stage (mice = E13, rats = E15, humans = 6wks) (Feldman and Bloch, 1978; Bloch et al., 1971; Weniger and Zeis, 1972). In humans the process of prostatic secretory cytodifferentiation occurs late in the second as well as in the third trimesters (Wernert et al., 1987; Xia et al., 1990). The overall process of secretory cytodifferentiation in the prostate is fundamentally similar to that occurring in other exocrine glands and will not be examined in this paper.

Early reports of human prostatic development are mostly based upon histologic studies published decades ago (Lowsley, 1912; Glenister, 1962; Andrews, 1951; Brody and Goldman, 1940). Unfortunately, there is not a single publication that describes all 5 stages of human prostatic development (Table 1). The pre-bud stage is illustrated in only 2 recent papers (Shapiro et al., 2004; Wang et al., 2001). The Shapiro et al paper deals with the germ layer origin of the prostatic utricle (Shapiro et al., 2004) with little emphasis on the pre-bud UGS, but otherwise is an excellent contribution on the prostatic utricle. The paper by Wang et al is the most detailed description of the pre-bud UGS, and reports the expression of a spectrum of keratins (KRT8, KRT18, KRT14, KRT5, & KRT19), as well as TP63 and GSTpi in pre-bud UGE at 9 weeks of gestation (Wang et al., 2001). The pre-bud UGE co-expresses an array of immunohistochemical markers indicative of both luminal and basal prostatic epithelial cells. During the course of prostatic development definitive luminal and basal prostatic epithelial cells differentiate and locate to their respective anatomic niches following canalization of the solid prostatic epithelial cords. Luminal epithelial cells lose basal cell markers, while retaining luminal markers. Likewise, basal prostatic epithelial cells lose luminal cell markers, while retaining basal epithelial cell markers (Wang et al., 2001).

The actual emergence of prostatic buds from the human fetal UGS is said to occur at 9 to 10 weeks of gestation: 9.5 weeks (Dauge et al., 1986), 10 weeks (Kellokumpu- Lehtonen et al., 1980), and in a 40-to 60-mm crown rump fetus (9 to 10 week) (Zondek and Zondek, 1979). The reported age range described above is likely due to the inherent difficulty of estimating specimen age as described below. During human prostatic development individual bilateral sets of prostatic buds emerge from specific locations from the UGS, and prostatic buds elongate along specific anatomical trajectories within urogenital sinus mesenchyme (UGM) (Timms et al., 1994; Timms, 2008; Timms and Hofkamp, 2011). Similar earlier observations led Lowsley to describe "lobar" subdivisions of the developing prostate (Lowsley, 1912). It is our interpretation that prostatic buds do not emerge synchronously, but instead form over

an extended time frame. Emerging buds can be first seen at ~10 weeks in humans, and additional budding appears to continue for several weeks. It is not known when the emergence of prostatic buds is finally complete, but we suspect that it is in the second trimester. It is also possible that several smaller buds may emerge but never develop into major ducts, but likely undergo regression because of temporal inductive differences.

Elongation and branching morphogenesis of human prostatic buds has been illustrated in several reports (Zhu et al., 2007; Adams et al., 2002; Dauge et al., 1986; Sebe et al., 2005; Xue et al., 2000; Wernert et al., 1987; Xia et al., 1990; Zondek and Zondek, 1979; Timms et al., 1994; Timms, 2008; Timms and Hofkamp, 2011). For many of these papers the analysis is exclusively histologic. These papers report morphology of solid epithelial cords or canalized prostatic ducts at various stages of development (Table 2). Photographs in the papers listed in Table 2 provide morphologic information on prostatic bud elongation, branching, canalization and secretory cytodifferentiation. As can be seen (Table 2), most of these studies deal with advanced stages of prostatic development, with the bulk of observations at 16 weeks and older when most of the prostate epithelium is in the form of canalized ducts undergoing secretory cytodifferentiation. Also in Table 3, reported data on epithelial differentiation markers are incomplete through the 5 stages of human prostatic development. A comprehensive ontogeny of epithelial differentiation markers encompassing bud elongation, branching, canalization and secretory cytodifferentiation will be presented in this paper.

Prostatic epithelium contains at least 3 classes of cells: luminal epithelial cells, basal epithelial cells and neuroendocrine cells. Luminal and basal prostatic epithelial cells each express a unique set of keratins and other differentiation markers (Wang et al., 2001). Neuroendocrine cells, which comprise only a small proportion of total human prostatic epithelial cells, are also found in the human prostate and are derived from neural crest (Szczyrba et al., 2017). Neuroendocrine cells expressing serotonin and chromogranin A have been detected as early as 13 weeks of gestation, and by 25 weeks neuroendocrine cells were identified in all prostates examined (Szczyrba et al., 2017; Xue et al., 2000).

For all species examined (including human), prostatic development is dependent upon androgens. Reports of androgenic effects on the human fetal prostate appear in only 3 papers. Human fetal prostates have been grown in organ culture in the presence and absence of androgens (Kellokumpu-Lehtinen et al., 1981; Kellokumpu-Lehtinen and Pelliniemi, 1988). In these studies the authors reported ultrastructural features of the epithelium and associated mesenchyme. Unfortunately, the potential androgenic induction of prostatic buds was not addressed. Zondek had the unique opportunity of studying a prostate from an ancephalic fetus. The focus in their paper was squamous metaplasia within the developing human prostate, which they proposed was due to a balance between estrogen and androgen action. They suggested "that diminished androgen production (due to ancephaly) led to a disturbance in the hormonal balance and was thus at least partly responsible for the extreme metaplastic changes in the organ" (Zondek and Zondek, 1979).

Morphogenetic effects within the developing human prostate (like that in other animals) are mediated via androgen receptors (AR), which have been reported in human fetal prostate

(Adams et al., 2002; Majumder and Kumar, 1997; Aumuller et al., 1998; Letellier et al., 2007; Levine et al., 1996; Saffarini et al., 2013; Singh et al., 2014). These papers demonstrate the presence of AR in various stages of human prostatic development, but a complete ontogeny of AR from pre-bud to secretory cytodifferentiation is not to be found in a single publication. The most complete ontogeny of AR in the human fetal prostate was reported by Adams et al (2002), who examined prostates from 11.5 to 34 weeks of gestation. Expression of AR in prostatic stroma was consistently observed from as early as 11.5 weeks to term (Adams et al., 2002). Stromal AR is in keeping with paracrine effects of androgens on prostatic epithelial development (Cunha et al., 2004a). Epithelial AR was also seen in the urothelium of the prostatic urethra (UGE) as well as in prostatic luminal epithelial cells at 15 weeks and thereafter (Adams et al., 2002). Androgen receptors continue to be expressed in epithelial and stromal cells in xenografts of human fetal prostates (Saffarini et al., 2013). A detailed ontogeny of AR expression from the pre-bud stage to advanced secretory cytodifferentiation is one of the topics of this paper.

While testosterone can activate androgen receptors in the UGS by directly binding to the AR, the more potent androgen, DHT, plays a critical role in prostatic development. DHT is produced within the developing UGS by the enzyme 5α-reductase, for which there are three isozymes, 5αRl, 5αR2 and 5αR3 (Russell et al., 1993; Russell and Wilson, 1994; Uemura et al., 2008; Li et al., 2011). DHT has a 10-fold greater affinity for the AR than testosterone (Deslypere et al., 1992). 5-alpha-reductase 2 is required for normal development of the prostate and male external genitalia (Andersson et al., 1991; Russell and Wilson, 1994). Prostates of patients with 5αR2 deficiency are rudimentary (Radmayr et al., 2008; Imperato-McGinley et al., 1992). 5-alpha-reductase 2 is predominantly expressed in prostatic mesenchyme (Radmayr et al., 2008; Levine et al., 1996). The function of 5αRl in urogenital development remains unclear. 5aR3 is associated with prostate cancer (Uemura et al., 2008; Li et al., 2011).

The development of the prostate is susceptible to effects of estrogens, and exogenous estrogens elicit a range of deleterious effects on the developing prostate in animal models (Prins et al., 2006). Development of the prostate is independent of estrogen receptors since the prostate is present in mice null for estrogen receptor alpha (ESR1), estrogen receptor beta (ESR2) and aromatase, an enzyme required for synthesis of estradiol (Eddy et al., 1996; Krege et al., 1998; Couse and Korach, 1999; Dupont et al., 2000; McPherson et al., 2001). Estrogen signaling is not required for prostatic bud patterning (Allgeier et al., 2010). Endogenous estrogens (primarily of maternal origin) elicit squamous metaplasia of the human fetal prostatic epithelium (Zondek and Zondek, 1979). Prostatic squamous metaplasia and other adverse effects have been reported in xenografts of human fetal prostates grown in mouse hosts treated with diethylstilbestrol (DES) or estradiol benzoate (Saffarini et al., 2015b; Saffarini et al., 2015a; Sugimura et al., 1988; Yonemura et al., 1995). Accordingly, ESR1 and ESR2 have been detected in the human fetal prostate (Adams et al., 2002; Shapiro et al., 2005). ESR1 was detected in prostatic luminal cells and in the stroma at 19 weeks of gestation and at 15 weeks in the prostatic utricle (Shapiro et al., 2005). ESR2 immunostaining was detected initially at 13 weeks in solid prostatic epithelial cords, and by 18 weeks intense ESR2 nuclear staining was seen in epithelium of canalized prostatic ducts

(Adams et al., 2002). Shapiro et al (2005) reported ESR2 immunostaining throughout the UGE and in the stroma at 7 weeks, which persisted in prostatic epithelium and stroma through 22 weeks.

The compilation of epithelial differentiation markers and signaling molecules in the human fetal prostate falls far short of that reported in mouse (Table 3). Letellier et al (2002) and Adams (2002) published the most comprehensive reports on this topic for the human fetal prostate. As above, a complete ontogeny of epithelial differentiation markers and signaling molecules from pre-bud to advanced secretory cytodifferentiation remains to be consolidated into a single publication.

Many of the earlier reports on human fetal prostatic development were published prior to the common use of color photographs, and on the whole, human prostatic development has been inadequately studied both at morphological and molecular levels. Experimental analyses utilizing xenografts detail effects of exogenous estrogens on human fetal prostatic development (Yonemura et al., 1995; Saffarini et al., 2013; Saffarini et al., 2015b; Saffarini et al., 2015a), but this experimental approach has been under utilized.

This review of the literature on human fetal prostate development emphasizes the need for a modern more complete treatment of this subject to provide a detailed ontogeny of human prostatic development from the pre-bud stage to advanced secretory cytodifferentiation that encompasses fetal prostatic gross anatomy, tissue morphogenesis (ductal budding, elongation, branching) and includes an ontogeny of selected differentiation markers and signaling molecules. To further explore androgen action in human prostatic development, we include preliminary xenograft studies that emphasize the value of this method for direct study the morphogenetic and molecular effects of androgens on the human fetal prostate.

Rodent prostatic development.

The current paradigm for prostatic development derives heavily from observations on embryonic mice and rats. The prostate and bladder develop from the urogenital sinus (UGS), the ventral division of the cloaca (Liaw et al., 2018; Yamada et al., 2003). The UGS, from which the prostate develops, is located immediately below the developing bladder. The bladder and future prostatic anlage become clearly demarcated by a constriction, immediately caudal to the junction of Wolffian ducts within the UGS (Fig. 1). For images of the freshly dissected mouse UGS with mesenchyme intact see our previojus publication (Staack et al., 2003).

Mouse and rat prostates form in five stages: pre-bud, bud initiation, bud elongation, branching morphogenesis and ductal canalization followed by differentiation of luminal and basal epithelial cells. In the pre-bud stage, that portion of the UGS destined to form prostate consists of a flattened tube of urogenital sinus epithelium (UGE) having a concave dorsal and a convex ventral surface surrounded by urogenital sinus mesenchyme (UGM) (Fig. 2). More caudally the UGE is circular in outline.

The adult mouse (and rat) prostate is organized into several individual lobes (ventral, dorsal, lateral and anterior prostate) (Sugimura et al., 1986c; Hayashi et al., 1991), and during

prostatic development solid epithelial buds arise from the UGE in a bilaterally symmetrical pattern indicative of the adult prostatic lobes (Timms et al., 1994; Timms, 2008). In the mouse and rat each prostatic lobe forms from 2 to several individual buds per side (Fig. 3). The mechanism of prostatic bud initiation is poorly understood, but is induced in response to fetal testicular androgens and is initiated via signals from the surrounding UGM (Cunha et al., 1987; Marker et al., 2003). In the pre-bud stage, androgens stimulate bands of *Edar, Nkx3–1,* and *Wnt10b* mRNAs to appear in anterior, ventral, and dorsolateral prostatic budding zones. These mRNAs are later focally restricted during bud initiation and elongation to nascent prostatic bud tips (Keil et al., 2014a; Sciavolino et al., 1997; Bieberich et al., 1996). Prostatic bud initiation is stochastic, and cords of UGS epithelium emerge and recede throughout the budding process. In response to androgens selected buds are stabilized as a result of activating WNT beta-catenin, which subsequently permits elongation of buds within prostatic budding zones while inhibiting buds elsewhere (Mehta et al., 2013; Allgeier et al., 2010). Prostatic bud number varies little between individual mice, suggesting a tightly regulated process (Lin et al., 2003). Nonetheless, mouse prostatic bud patterns are disrupted by estrogenic chemicals, anti-androgens, plasticizers, and environmental contaminants, which can increase or decrease bud number in a dose-dependent fashion (Timms et al., 1999; Moore et al., 2001; Timms et al., 2005; Lin et al., 2003; Donjacour and Cunha, 1988). Whether these chemicals also interfere with human prostate development has not been determined, but xenograft studies have shown that exogenous estrogens affect histodifferentiation of developing human prostate and change the histological pattern of prostate ducts (Saffarini et al., 2015b; Sugimura et al., 1988; Yonemura et al., 1995).

Elongating prostatic buds have two extremities: (a) Their proximal attachment to the urogenital sinus/prostatic urethra and (b) their distal tip. During "ductal elongation" DNA synthesis is vastly higher at the distal tips versus proximal regions of the elongating prostatic buds in the developing mouse prostate (Sugimura et al., 1986d). Prostatic bud elongation is controlled by intrinsic and extrinsic factors. DNA methylation status of E- cadherin is an example of an intrinsic bud elongation mechanism. DNA methylation of the E-cadherin promoter during the pre-bud stage and continuing through bud initiation reduces E-cadherin transcription and increases bud epithelial cell motility (Keil et al., 2014b). Extrinsic chemotactic factors also participate in prostatic bud elongation, as they do in other tissues (Park et al., 1998; Weaver et al., 2000). Mouse and rat prostatic bud elongation is determined in part by fibroblast growth factors 7 and 10 and other growth factors expressed by mesenchymal condensates (also known as mesenchymal pads) in peripheral UGM (Timms et al., 1994; Timms et al., 1995; Georgas et al., 2015; Sugimura et al., 1996; Thomson and Cunha, 1999; Donjacour et al., 2003; Kuslak et al., 2007; Kuslak and Marker, 2007). It is unknown whether DNA methylation status influences human prostatic bud elongation, or whether human male UGS is characterized by *FGF10* expressing mesenchymal condensates.

Branching morphogenesis within exocrine glands is an extremely complex process that has been extensively studied in a variety of organs (salivary gland, mammary gland, lung, kidney, etc.) (Blake and Rosenblum, 2014; Iber and Menshykau, 2013; Ochoa-Espinosa and Affolter, 2012; Patel et al., 2006; Sternlicht et al., 2006; Wang et al., 2017). Branching morphogenesis occurs at the solid tips of elongating prostatic buds where DNA synthesis is highest. In mice and rats the patterns of ductal branching morphogenesis are unique for each

lobe of the prostate (Sugimura et al., 1986b; Hayashi et al., 1991). The ventral prostate has a branching pattern similar to that of an elm tree with a short main duct and profuse branching thereafter, whereas the branching pattern of the dorsal-lateral prostate is more like that of a palm tree with long main ducts emerging from the prostatic urethra and branches occurring far distal to the urethra.

The detailed literature on morphogenesis of the prostate in rats and mice coupled with recent advances in the cellular and molecular mechanisms of prostatic development in laboratory animals provide the conceptual and biologic framework for future studies on development of the human prostate, a topic of considerable importance with clinical implications. Benign prostatic hyperplasia (BPH) in humans is one of the major health problems that afflict a high percentage of men as they age. A common feature shared during fetal prostatic development and as well as during the pathogenesis of BPH is the neo-formation of ductal-acinar architecture, an idea annunciated many years ago by John McNeal (McNeal, 1978). The vast literature on prostatic development in laboratory animals serves as a guide for detailed examination of human prostatic development. For the first time this paper provides a compendium on human prostatic development from the pre-bud stage to advanced secretory cytodifferentiation that encompasses fetal prostatic gross anatomy (Shen et al., 2018a), tissue morphogenesis (ductal budding, elongation, branching) and includes an ontogeny of selected differentiation markers and signaling molecules. It is hoped that this paper will stimulate future studies on this important topic.

Materials and Methods

Human fetal prostates were collected from abortus specimens devoid of patient identifiers after elective termination of pregnancy (Committee on Human Research at UCSF, IRB# 12–08813). Given that current surgical procedures are disruptive, the initial challenge in human prostate development is finding the fetal prostate in the abortus specimen. The bladder and prostate complex can be found due its distinctive gross morphology (Fig. 4) (Shen et al., 2018a). It is especially important to examine the proximal end of the umbilical cord, as sometimes the bladder and prostate are attached. In other cases an intact pelvis containing the bladder and prostate can be found. Gestational age of disrupted surgical specimens can be estimated using heel-toe length (Drey et al., 2005). Ages of the human prostatic specimens that were fixed in formalin and processed for histology and immunohistochemistry are: 9.5, 10.5 (2), 11 (3), 11.5, 12 (5), 12.5 (2), 13 (4), 14 (3), 14.5 (2), 16 (3), 17 (2), 17.5, 18, 19, 19.5, 20 and 21 weeks of gestation (numbers in parentheses indicates number of specimens at the specified age). Alternatively, crown-rump measurements can be used (Robboy et al., 2017) if intact specimens are available.

It is important to appreciate that gestational timing of the human embryos (and fetuses) is in the final analysis derived from patient interviews, even though information concerning the last menstrual period is typically inaccurate, especially for second trimester abortions. In this regard, a quote from the Carnegie embryo collection website is most informative. "An embryo is assigned a Carnegie stage (numbered from 1 to 23) based on its external features. This staging system is not dependent on the chronological age or the size of the embryo. The stages are in a sense arbitrary levels of maturity based on multiple physical features.

Embryos that might have different ages or sizes can be assigned the same Carnegie stage based on their external appearance because of the natural variation which occurs between individuals (Smith, 2016)". Historically, most abortions involved vaginal delivery of intact embryos/fetuses from which crown-rump measurements were used as a gauge of gestational age (Streeter, 1951). Today, crown- rump measurements are rarely useful as current abortion procedures disrupt overall specimen integrity. Accordingly, heel-toe length has been used to determine fetal maturity, which gives a rough estimate of age (Drey et al., 2005). As the Carnegie Collection literature advocates, gross images ordered by increasing size and morphological complexity is more important than exact estimate of age (Shen et al., 2018a). With this in mind, it should be recognized that actual embryonic/fetal ages in individual papers are clearly estimates of questionable accuracy. Table 1 presents a timeline of human prostatic development, and the ages given for human specimens are best approximations. More important are the biological events that occur during these stages of prostatic development.

Human fetal prostates 7 to 21 weeks of gestation were collected in ice cold saline, fixed in 10% buffered formalin and serially sectioned at 7μm. Every 20th section was stained with hematoxylin and eosin (H&E) to assess histology. Intervening paraffin sections were immunostained with antibodies to a variety of proteins as described previously (Rodriguez et al., 2012) (Table 4). Immunostaining was detected using horseradish peroxidase-based Vectastain kits (Vector Laboratories, Burlingame, CA). Alternatively, immunoflourescent methods were used as described previously (Shen et al., 2015). For negative controls the primary antibodies were deleted. This study is based upon analysis of 25 fixed human fetal specimens 9 to 21 weeks of gestation. In addition, 4 human fetal prostates at 13 and 14 weeks of gestation and 11 female bladders/urethras at 10.5 to 14 weeks of gestation were collected for xenograft studies described below.

For xenograft studies human fetal prostates were surgically isolated from the bladder and the pelvic urethra and then transected in the midline to yield right and left halves which were transplanted under the renal capsules of male athymic nude mice (CD- 1 NU/NU, Charles River Laboratories, Wilmington, MA) as previously described (Cunha and Baskin, 2016). The IACUC committee at UCSF approved all grafting procedures. The mouse hosts were castrated at the time of transplantation, and the hosts either received a 20mg pellet of dihydrotestosterone (DHT) (A8380, Sigma-Aldrich, St. Louis, MO, USA) or were untreated (sham). Our selection of DHT instead of testosterone eliminates the possibility of aromatase-mediated conversion of testosterone to estradiol. Grafts were grown for 1 to 2 months, at which time the hosts were euthanized, and the grafts harvested. Grafts were fixed in 10% neutral buffered formalin for 48 hours, embedded in paraffin, and serially sectioned at 7μm. Every 20th section was stained with H&E to highlight tissue architecture. Intervening sections were immunostained with a variety of primary antibodies (Table 4).

A 12 week human fetal prostate was processed using Light Sheet™ microscopy and double immunostained with antibodies to E-cadherin to reveal epithelium and S100 to reveal neurons and glia as described previously (Vives et al., 2003).

Segments of human fetal female urethra immediately below the bladder, which is considered to be anatomically homologous to the prostatic urethra, were also grafted into castrated male hosts that were either untreated (N=4) or DHT-treated (N=5) to determine whether DHT could induce prostatic development in the female urethra. After 4 or 8 weeks of in vivo growth, the grafts were harvested and processed as above for histology and immunohistochemistry.

C. Results

A. Gross anatomy.

Figure 4 presents the gross anatomy of human fetal prostates from 13 to 21 weeks. The prostate is recognized as a distinct bulge immediately below the bladder. Outer edges of the prostate present a smooth contour, even though extraneous connective tissue was frequently present as well (Fig. 4). This extraneous tissue (when present) frequently contained pelvic ganglia and neuronal processes (Figs. 10D & 17). The wholemount images in figure 4 will be useful for future investigators in identifying human fetal prostates. When an intact pelvis is obtained, it is useful to dissect the combined bladder-prostatic complex.

B. Histology.

Development of the human prostate (like that of the mouse) is appropriately subdivided into the following sequential stages: (a) Pre-bud stage, (b) Initial budding, (c) Bud elongation and branching, and (d) Ductal canalization (Table 1). In adulthood most human prostatic ducts open into the urethra near the verumontanum (Fig. 5), reflecting the fact that human fetal prostatic buds emerge in the region of the verumontanum where the Wolffian ducts (WD) and the fused Mullerian ducts (prostatic utricle) join the UGS (prostatic urethra) (Figs. 6, 7 & 9). Figure 6 displays transverse sections through the verumontanum of the urogenital sinus (UGS) of a 9-week pre-bud male fetus immunostained for Foxal (Fig. 6A), Pax2 (Fig. 6B), TP63 (Fig. 6C) and androgen receptor (Fig. 6D). Within organs and organ rudiments of the urogenital system within the pelvis and perineum Foxal is an endodermal marker (Diez-Roux et al., 2011; Robboy et al., 2017; Besnard et al., 2004), which stains urogenital sinus epithelium (UGE) (Fig. 6A), as well as developing epithelia of the bladder, pelvic and penile urethras, rectum and anal canal (Robboy et al., 2017; Shen et al., 2018b). Pax2 stains epithelium of the WDs and prostatic utricle derived from the Mullerian epithelium (Fig. 6B). Note that Pax2-positive epithelial cells contribute to the lining of the human prostatic urethra (verumontanum) (Fig. 6B). This is a noteworthy difference from the mouse in which a tuft of Foxa1-positive endoderm-derived UGE separates the Foxa1- positive UGE from Pax2-positive WD epithelium (Joseph et al., 2018). TP63 is expressed in basal epithelial cells of the UGS, but not in epithelium of the WDs and prostatic utricle (Fig. 6C). Androgen receptor is expressed in urogenital sinus mesenchyme (UGM), in luminal cells of the UGE and in WD epithelium, but not in the prostatic utricle (Fig. 6D). The epithelium lining the 9-week UGS and covering the verumontanum is multilayered, and expresses a spectrum of differentiation markers (Table 5). In keeping with the endodermal origin of UGE, FOXA1 is expressed in pre-bud UGE (Fig. 6A). Keratins 7 (Fig. 7A), 8 (Fig. 7B) and the androgen receptor (AR, Fig. 6D) are expressed in apical layers of the UGE, while keratin 6 (Fig. 7A) and TP63 (Fig. 6C) are expressed predominantly in basal layers. Keratin 19 is expressed

throughout the full UGE thickness (Fig. 7C). Uroplakin and keratins 10, 14 and 15 are not expressed in the pre-bud UGE (not illustrated). The Mullerian epithelium of the prostatic utricle is negative for Foxa1 (Fig. 6A), TP63 (Fig. 6C) and AR (Fig. 6D), but reactive for Pax2 (Fig. 6B).

The mouse colliculus seminalis or verumontanum is perhaps the least well- described anatomical feature in the male reproductive tract. Substantial differences exist between the verumontanum of human versus mouse. In both species the verumontanum is associated with the prostatic urethra. In the adult mouse, the verumontanum is encircled by a thick layer of striated muscle, known as the rhabdosphincter (Green, 1966; Nicholson et al., 2012) (Fig. 8A). In the adult human prostate a similar sphincter of striated muscle composition has been described, but is located distal to the verumontanum, and is discontinuous and meager (McNeal, 1981). Thus, the rhabdosphincter is much more highly developed in mice versus men. The prostatic utricle is present during prostatic development in both human and rodent species (Figs. 6–7 & 9A) (Timms, 2008; Timms and Hofkamp, 2011), and in humans the prostatic utricle is retained into adulthood opening onto the apex of the verumontanum (Clemente, 1985). A prostatic utricle is also present in the adult mouse (Li et al., 2001), but its connection to the adult prostatic urethra has not been described to our knowledge. In humans, the ducts of the bilateral seminal vesicle joins the vas deferens to form the paired ejaculatory ducts that traverse the prostate to open with the prostatic utricle at the apex of the verumontanum (Clemente, 1985) (Fig. 5B). Fusion of the seminal vesicle ducts with the vas deferens to form the ejaculatory ducts has been reported in mouse embryos (Timms and Hofkamp, 2011; Lin et al., 2003). However, the Biology of the Laboratory Mouse (Green, 1966) (http://www.informatics.jax.org/greenbook/frames/frame13.shtml) contains a histological section showing the bilateral vas deferens and bilateral ducts of the seminal vesicle opening separately into the prostatic urethra at the verumontanum. Our recent examination of the adult C57bl6 adult mouse verumontanum demonstrates the paired vas deferens and ducts of the seminal vesicle open separately at the tip of the verumontanum in some adult mice, while in other adult mice of the same strain paired ejaculatory ducts open into the prostatic urethra on the verumontanum (Fig. 8B), meaning that the vas deferens and ducts of the seminal vesicles have joined prior to opening at the tip of the verumontanum. Whether ejaculatory ducts are present or absent in other mouse strains remains to be determined. Therefore, although homology exists in the verumontanum between mouse and human, distinct anatomical differences are evident.

Human prostatic bud initiation occurs at 10 to 11 weeks of gestation with the appearance of solid epithelial buds that emerge from different quadrants of the human prostatic urethra over a considerable cranial to caudal distance in the region of the verumontanum (Figs. 9– 10). The pattern of emergence of human (and mouse and rat) prostatic buds (Fig. 9) has been studied previously, and three-dimensional reconstruction studies suggestion a distinct developmental pattern of emergence of mouse and human prostatic buds (Fig. 9), which directly relates to the adult pattern of prostatic ducts (Fig. 5) (Sugimura et al., 1986b; Timms, 2008; Timms and Hofkamp, 2011). Figures 9 and 10 show that human prostatic buds emerge from the urethra in the region of the verumontanum, which can be identified by the presence of the prostatic utricle and ejaculatory ducts (Figs. 9B & 10). Figures 10A & B show branched prostatic buds of varying length emerging from the lateral aspect of the

verumontanum. A rich neuronal network is associated with the developing prostate and bladder (Fig. 10D).

Homologies between human and mouse prostatic lobes/zones continue to be a subject of speculation and debate (Shappell et al., 2004). One major difference between mouse and human prostate is the ventral prostate, which is present in mice and rats and absent in humans (See Figs. 5B, 8C & 10A-B) (Lee et al., 2011). The mouse anterior prostate (Fig. 9A) appears to be homologous to the human central zone, and the mouse dorsal and lateral prostates (Fig. 9A) are likely homologues of the human peripheral zone (Lee et al., 2011) even though a solid consensus on mouse/human lobe/zone homology remains unclear (Shappell et al., 2004). Zonal morphology of the human prostate is derived from the work of John McNeal (McNeal, 1981).

Epithelial proliferation appears to play an important role in emergence of human prostatic buds. Ki67 expression is clearly elevated at the tips of emerging prostatic buds relative to the UGE from which they emerge (Fig. 11). Figure 11A shows many buds on the ventral surface of the UGE at 12 weeks of gestation (versus fewer buds on the dorsal and lateral surface of the UGE). However, such ventrally emergent ducts are not present in adulthood (McNeal, 1981), and instead prostatic ducts drain into the lateral and dorsal aspects of the prostatic urethra (Fig. 5) (Timms, 1997). In mice the tips of elongating prostatic ducts exhibit highest levels of DNA synthesis (Sugimura et al., 1986d).

The solid prostatic buds emerging from the UGE mostly express the same differentiation markers seen in the UGE prior to bud emergence (Table 5). Initiation of bud formation, which starts at about 10–11 weeks postnatal, appears to continue over an extended period based upon cursory analysis of serial sections of human fetal prostates >12 weeks of gestation. Newly emerged solid prostatic buds extend into the surrounding UGM. Bud elongation initially generates unbranched solid epithelial cords that subsequently undergo branching and canalization.

Prostatic bud elongation, branching and canalization are processes that occur simultaneously over many weeks beginning at about 12 weeks of gestation, and evidence suggests that ductal branching patterns are different in individual prostatic "lobes". Lowsley (1912) identified five separate lobes of the human fetal prostate, and in rats and mice 4 distinct prostatic lobes are recognized (ventral, dorsal, lateral and anterior) (Figs. 3 & 9A). Rodent prostatic ductal branching patterns vary considerably between individual prostatic lobes (Sugimura et al., 1986b; Hayashi et al., 1991). Thus, in laboratory rodents the distance from the prostatic urethra to the first ductal branch point is short for the ventral prostate and considerably longer for the dorsal and lateral prostates (Sugimura et al., 1986b; Hayashi et al., 1991). We suspect that this is also true for human prostate, an idea supported by two observations: (a) Measurements from serial sections of the distance from the prostatic urethra to the first branch point is short in some areas (~250μm) (Fig. 12A). (b) Thick (0.5mm) coronal sections of human fetal prostate reveal ducts with an initial branch point ~1000μm from their origin from the urethra (Fig. 12B). This ~4-fold difference in ductal length to the first branch point is consistent with the idea that human ductal branching

patterns may be lobe specific as is the case for mice and rats. Further studies are required to definitively resolve this question.

Elongation of human prostatic ducts occurs principally via cell proliferation that is concentrated/enhanced at/near the solid ductal tips as is also the case for developing mouse prostate (Sugimura et al., 1986d), even though Ki67-labeled epithelial cells are observed along the full length of developing human prostatic ducts from their origin at the urethra to their distal tips (Fig. 11). Enhanced Ki67 labeling was observed consistently in solid epithelial buds or solid epithelial cords in developing human fetal prostates over the time frame of 12 to 19 weeks. While this was not quantified, our observations were consistent from specimen to specimen. Four specimens were examined for Ki67 labeling (12 to 19 weeks) and all showed elevated Ki67 labeling at the tips of the solid epithelial cords, while Ki67 labeling was reduced in canalized ducts closer to the prostatic urethra (Fig. 11B-D). This observation fully corroborates similar observations from mouse prostatic development (Sugimura et al., 1986d).

From 12 weeks onward prostatic buds are elongating, branching and canalizing to yield luminized ducts composed of a continuous layer of basal epithelial cells and a continuous layer of columnar luminal cells. In mice and rats, basal cells form a discontinuous layer (Hayward et al., 1996b). By 19 weeks of gestation fully canalized ducts exhibit a high degree of differentiation. Luminal epithelial cells express keratins 7, 8 and 19, Runxl and androgen receptor, while basal epithelial cells express keratin 6, Runxl and TP63 (Fig. 13). Surprisingly, keratin 14 immunostaining was rarely detected in human fetal prostatic basal cells in specimens up to 19 weeks (not illustrated). Keratin 14 is a feature of adult prostatic basal cells (Hudson et al., 2001). We believe that the unexpected absence of keratin 14 immunostaining in developing human prostatic ducts is a function of differentiation state of the epithelium. Finally, uroplakin was expressed in epithelium of the prostatic urethra and in proximal aspects of canalized ducts near the urethra, but not in prostatic ducts distal to the urethra (Fig. 14A).

The gradual process of ductal elongation, branching and canalization occurs from week 12 onward and is initiated proximally at the urethra and progresses distally along the ducts. Thus, from 12 to 19 weeks canalized ducts transition to solid epithelial cords at some point along their proximal to distally axis (Fig. 14). In the course of proximal to distal canalization, epithelial marker expression changes at the canalized-solid interface. The distal portions of solid epithelial cords retain a similar pattern of marker expression seen in pre-bud UGE (Table 5). In contrast, canalized ducts exhibit the highly differentiation state described above. Intermediate patterns are seen at the canalized-solid interface. For example, uroplakin, which is prominently expressed in urethral epithelium, is seen in central cells of solid epithelial cords near the urethra (Fig. 14A). Keratins 7, 8 and 19, characteristic markers of luminal cells, are seen in central cells of solid epithelial cords (Fig. 14B & G). TP63 is normally expressed in basal cells of canalized ducts (Figs 13F and14C) and is expressed throughout solid epithelial cords (Fig. 14C), but near the canalized-solid interface, central cells are devoid of TP63. Such TP63-negative cells are believed to be differentiating luminal cells. A similar pattern is seen in regard to keratin 6 (Fig. 14D). Androgen receptor, which is normally confined to luminal cells, is absent in solid epithelial cords. This marker is turned

on precisely at the canalized-solid junction (Fig. 14E & F). The pattern of expression of Runxl (Fig. 14H) at the canalized-solid junction is similar to that of AR (Fig. 14E-F).

Differentiation of smooth muscle.

α-Actin is one of the earliest in a series of differentiation markers of smooth muscle, but also is expressed in myofibroblasts (Darby et al., 1990) and myoepithelial cells (Gugliotta et al., 1988). α-Actin is expressed in smooth muscle that develops within the bladder (Liaw et al., 2018), prostate (Hayward et al., 1996c) and the urethra (Sebe et al., 2005), and thus α-actin was used to detect smooth muscle precursors and smooth muscle within the developing human prostate. At 9 weeks of gestation smooth muscle α- actin is sparsely expressed in peripheral ventral-lateral UGM (Fig. 15A). Continuing this trend, at 14 weeks α-actin-positive smooth muscle bundles are seen in the ventral UGM and sparsely in dorsal UGM (Fig. 15B). At 19 weeks a continuous layer of α-actin- positive smooth muscle extends around the entire circumference of the UGM where solid epithelial cords are branching (Fig. 15C). Thus, distal ductal branching of the solid epithelial cords occurs peripherally in regions rich in smooth muscle. At 19 weeks the urethra and most of the central portion of the UGM is relatively deficient in a-actin- positive smooth muscle. Given that adult prostatic stroma is mostly composed of smooth muscle (McNeal, 1983), this means that human prostatic stroma is only partially differentiated at 19 weeks.

Xenograft studies

Human fetal prostates ranging in age from 13 to 14 weeks were bisected into right and left halves, and the pieces grafted into castrated male nude mice that were either untreated (N=4) or treated by a subcutaneous 20mg pellet of dihydrotestosterone (DHT) (N=4). At 13 and 14 weeks of gestation prostatic ducts were present prior to grafting. However, following 4 weeks of growth in the nude mice the number of ducts observed the DHT-treated grafts was strikingly elevated relative to the androgen-deficient control group (4/4) (Figs. 16A1 versus 16B1). Androgen receptor expression was strikingly enhanced in DHT-treated versus androgen-deficient control specimens (4/4) (Figs. 16A2 versus 16B2). In DHT-treated human fetal prostate grafts, AR was broadly expressed in both stromal and epithelial cells (Fig. 16A2), while in androgen-deficient control grafts AR was undetectable in prostatic ducts and the associated stroma, but was present in peripheral stroma (4/4) (Fig. 16B1 & 16B2). In addition, ducts in the DHT-treated group consistently exhibited a higher degree of epithelial differentiation compared to that seen in the control group in regard to expression of TP63, keratins 7, 8 and 19 (4/4) (Fig. 17A-D). Keratin 14 was not detected in either solid epithelial cords or canalized prostatic ducts of human fetal prostatic grafts grown in either control or DHT-treated hosts. Patterning of α-actin-positive smooth muscle was also affected by DHT (Fig. 17E). Table 6 provides a comparison of marker expression in DHT-treated and control human fetal prostatic xenografts. Surprisingly, neurons within ganglia and neuronal processes were seen in grafts grown in both DHT-treated and control hosts (Fig. 17F1 & 17F2). The presence and amount of neurons within ganglia and nerve fibers may not be related to the presence/absence of DHT, but may depend upon whether ganglion cells survived the dissection and grafting processes. Nonetheless, the important point is that ganglion cells and nerve fibers can be studied in this xenograft model.

NKX3.1 was not observed in solid prostatic epithelial cords whose development was arrested due to androgen-deficiency in grafts grown for 4 weeks in untreated castrated hosts (N=3/3) (Fig. 18A). Human fetal prostatic xenografts grown in DHT- treated hosts for 4 weeks exhibited ductal canalization and advanced glandular differentiation (Figs. 16–17), and at least some of the "mature" luminal prostatic epithelial cells were reactive for NKX3.1 (Fig. 18B). This observation suggests that the expression of NKX3.1 in developing human prostate is androgen-dependent and requires advanced differentiation of luminal cells.

Finally, to develop a model of de novo human prostatic morphogenesis/differentiation, the segment of the human fetal female urethra immediately below the bladder (homologue of the prostatic urethra) was grafted into castrated DHT-treated hosts (N=7) and untreated castrated hosts (N=4) (Fig. 19A). This region of the female urethra consists of a multi-layered urothelium with associated epithelial projections into the surrounding stroma (Fig. 19B). Following 4 or 8 weeks of in vivo growth, human female urethral grafts treated with DHT (7/7) contained an abundance of prostate-like solid epithelial cords and canalized ducts (Fig. 20A). The typical range of prostatic epithelial markers was observed: KRT19 (Fig. 20A) was expressed in urethral and prostatic epithelial cells. KRT7 (Fig. 20B) and KRT8 (not illustrated) were expressed in prostatic luminal cells and in central cells of solid epithelial cords. KRT14 was not expressed (not illustrated) (Table 6). TP63 (Fig. 20C) was expressed in basal cells of urethral epithelium, in canalized ducts and uniformly throughout the solid epithelial cords. The androgen receptor immunohistochemical profile of DHT-treated grafts of human female fetal urethra (Fig. 21A-B) was identical to that of xenografts of DHT-treated human fetal prostate (Fig. 16) as well as non-grafted human fetal prostatic specimens as described above (Figs. 13D & 14E-F). In DHT-treated xenografts of human fetal female urethras, nuclear AR was observed broadly throughout the stroma, as well as in luminal epithelial cells (Fig. 21A-B). NKX3.1 (Fig. 21C) was expressed in epithelial cells of canalized ducts of DHT-treated female urethral grafts, but not in solid epithelial cords. A similar pattern of NKX3.1 immunostaining has been reported for developing mouse prostate (Maho Shibata and Michael Shen, personal communication). In mice NKX3.1 is a marker expressed in developing and adult prostate and is absent in embryonic female UGE, but present in male mouse UGE (Bhatia-Gaur et al., 1999). Finally, grafts of human female urethra grown in DHT-treated hosts expressed human prostate specific antigen (PSA) and prostatic acid phosphatase (Fig. 22), known markers of human prostatic epithelium (Dema and Tudose, 1998; Lam et al., 1989). Expression of NKX3.1, prostate specific antigen and prostatic acid phosphatase was only observed in canalized ducts exhibiting advanced epithelial differentiation (Figs. 21 and 22). Thus, xenografts of human fetal female urethra treated with DHT undergo prostatic differentiation.

Comparable control xenografts of human fetal female urethras (4/4) grown in untreated castrated hosts maintained a urethra-like structure with associated solid epithelial buds, which were rarely canalized (Figs. 20 & 21). Keratin 19 was expressed in the retained urethral epithelium and in solid epithelial cords of control specimens (Fig. 20D). Keratins 7 (Fig. 20E) and 8 (not illustrated) had a similar expression profile and were expressed in urethral epithelium, in solid epithelial cords and in centrally located epithelial cells of solid epithelial cords. TP63 was expressed throughout solid "ducts" in both DHT-treated and control xenografts (Fig. 20F), and in basal epithelial cells of canalized ducts (Fig. 20F). In

the absence of androgens (control xenografts) the solid (and the rare canalized) epithelial cords were AR-negative, with rare AR-reactive stromal cells (Fig. 21D & E). NKX3.1 was not detected in human fetal female urethral xenografts grown in androgen-deficient control hosts (Fig. 21F) and prostate specific antigen and prostatic acid phosphatase was not detected (not illustrated). Taken together, prostatic differentiation was induced by DHT in human fetal female urethral xenografts and was absent in androgen-deficient control xenografts (Table 6).

Discussion

Biologic and molecular mechanisms of human prostatic development are clearly relevant to the pathogenesis of benign prostatic hyperplasia (BPH) and prostate cancer (PRCA). An important feature shared in normal prostatic development and pathogenesis of BPH and prostate cancer is the neoformation of ductal-acinar architecture. Implicit in this statement is the role of epithelial-stromal interactions, regulation of epithelial proliferation, hormone action, epithelial differentiation and the underlying molecular mechanisms operative in both normal prostatic development and pathogenesis (Olumi et al., 1999; Cunha et al., 2002; Cunha et al., 2004b; Marker et al., 2003; Ricke et al., 2012; Ricke et al., 2008; Ricke et al., 2016; Nicholson et al., 2012; Nicholson et al., 2015). While the field of mouse prostatic development has advanced considerably, studies of human prostatic development are significantly under-represented in the literature and in many cases based upon old technology. While mice and humans share many aspects of prostatic development, human prostatic development and adult anatomy differ from that of mouse. Accordingly, a thorough comparison of the molecular landscape between developing mouse and human prostate has not been possible because the human fetal resources for such a comparison have been limited, and in no case has the expression of genes/proteins been followed temporally through the five distinct phases of human prostatic development. Accordingly, the goal of this paper is provide guidelines on how to isolate human fetal prostate and to describe the developmental process through the 5 stages of development: (a) pre-bud UGS, (b) emergence of solid prostatic epithelial buds from UGE, (c) bud elongation and branching, (d) canalization of the solid epithelial buds, (e) differentiation of luminal and basal epithelial cells, and (f) secretory cytodifferentiation. To this end, we present the histogenesis of the human prostate as well as a limited number of differentiation and molecular markers assessed by immunohistochemistry. Additionally, we illustrate findings based upon xenograft studies that shed light on the cellular basis of human prostatic development, which will be key to future mechanistic studies. This study, in conjunction with the earlier literature, should advance understanding of human prostatic development and its relevance to human prostatic pathogenesis. Finally it is important to utilize recent advances in the molecular mechanisms of prostatic development in mice as a guide to future mechanistic studies in human prostatic development, and to understand both the developmental and molecular similarities as well as differences in human versus mouse prostatic development.

A distinctive anatomical feature in human prostate development is the verumontanum, which is an elongated dorsal prominence projecting into the prostatic urethra. Three structures open into the human prostatic urethra at/near the apex of the verumontanum, namely the prostatic utricle (derived from the fused Müllerian ducts) flanked by the paired ejaculatory ducts

(derived from the Wolffian ducts) (Clemente, 1985; Shapiro et al., 2004; Zondek and Zondek, 1979; 1980). Comparable structures (verumontanum, prostatic utricle and ejaculatory ducts) have been reported during mouse prostatic development (Timms et al., 1994). However, the adult mouse verumontanum differs substantially from its human counterpart in several respects: (a) the rhabdosphincter of skeletal muscle is much more developed in mice versus men, (b) in humans the paired vas deferens and bilateral ducts of the seminal vesicle join to form ejaculatory ducts that traverse the prostate before emptying into the prostatic urethra, (c) in mice the ejaculatory ducts (when present) are very short, joining together near the tip of the verumontanum. The surface epithelium of the verumontanum in both humans and mice is derived from the endodermal epithelium of the UGS, an idea confirmed by Foxa1 immunostaining (Fig. 6A). The WDs and prostatic utricle are PAX2-positive, thus confirming an earlier report (Shapiro et al., 2004). Thus, the apex of the human verumontanum represents a junction between endodermal epithelium of the UGS and mesodermal epithelia of the Wolffian and Mullerian ducts. Examination of figure 6B demonstrates that epithelial cells of Wolffian duct origin populate a restricted patch of verumontanum surface epithelium. An alternative possibility is that some endoderm- derived cells lose FOXA1 and acquired PAX2 expression in this region. How this mixing of epithelia occurs, modulates with age and/or persists into adulthood and responds to injury remains to be determined. While Wolffian and Mullerian ducts are both derived from mesoderm, Wolffian duct epithelium is AR-positive, while Mullerian epithelium of the prostatic utricle is not (Fig. 6D).

In rodents, the epithelia of the verumontanum and prostate are estrogen sensitive. In humans this is manifest as squamous metaplasia attributed to high levels of maternal estrogens (Zondek and Zondek, 1979), which can also be elicited by exogenous estrogens (DES or 17β-estradiol) in human fetal prostatic xenografts (Saffarini et al., 2015b; Sugimura et al., 1988; Yonemura et al., 1995). Estrogens, including 17β-estradiol (E2), ethinyl-E2 (EE2), diethylstilbestrol, and bisphenol-A have been shown to enlarge the verumontanum and alter other aspects of prostate growth in laboratory animals (Timms et al., 2005; vom Saal et al., 1997). Additionally, estrogens and other factors can developmentally alter the prostatic anatomy, epigenetics, and gene signatures, which may have adverse consequences in adulthood (Timms et al., 2005; Taylor et al., 2011; Ricke et al., 2016; Taylor et al., 2012). Moving forward, assessing estrogen-induced changes in human prostate development will be key to elucidating the role of fetal exposure to hormones and endocrine disrupting chemicals to adult disease.

Mouse and human prostates are derived from endodermal UGE, even though only a restricted portion of the UGE is the site of prostatic development. This idea is emphasized in figures 1, 3, 9 and 10. In human prostatic development enduring prostatic ducts emerge from the UGS along the lateral sides of the verumontanum. Lowsley described 5 bilateral groups of prostatic buds (which he designated as lobes). One emerged from the ventral surface of the UGS. This so-called ventral lobe is not present in the adult human prostate (McNeal, 1981). Presumably, the ventral buds are transitory structures that form and then regress in the human prostate. Confirming Lowsley, we observed buds emerging from the ventral aspect of the human fetal UGS at 12 weeks of gestation (Fig. 11A), while at 14 weeks such ventral buds were not seen (Fig. 12A). Studies in mice have shown that prostatic bud

initiation is stochastic, and that prostatic buds emerge and recede during the budding process. Small epithelial outgrowths are observed in the absence of androgens, and functional androgen receptors are not required for bud initiation (Allgeier et al., 2010). The role of androgen and downstream signaling pathways is to support enlargement and elongation of buds in appropriate anatomical positions, while at the same time repressing buds that form in inappropriate positions (Mehta et al., 2013). The ontogeny of epithelial androgen receptors is initiated in central cells within the solid prostatic epithelial cords and then becomes localized to luminal prostatic epithelial cells within canalized ducts (Figs. 13, 14E-F, 16A2 & 21A-B), a process identical to that seen in rat prostatic development (Hayward et al., 1996a).

Human prostatic bud formation and elongation appear to be due to focal epithelial proliferation. Human prostatic buds emerging from the UGS are heavily labeled with Ki67 (Fig. 11A). During prostatic ductal elongation solid tips of ducts and solid prostatic epithelial cords are clearly more heavily Ki67-labeled than proximally situated canalized ducts (Fig. 11B-D). This pattern of enhanced proliferative activity at/near the ductal tips is in complete agreement with a remarkably similar pattern of DNA synthetic activity in the developing mouse prostate (Sugimura et al., 1986d). The basis of these regional differences in epithelial proliferative activity is presumably related to regional differences in the production of growth factors by UGM and possible regional differences in expression of growth factor receptors in the epithelium, an idea in need of detailed exploration in the developing human prostate. From studies in mice, proliferation of prostatic epithelium is elicited by androgens acting via mesenchymal androgen receptors (Sugimura et al., 1986a). This paracrine effect is elicited via growth factors such as FGF7 and FGF10 produced by UGM (Thomson and Cunha, 1999; Sugimura et al., 1996; Donjacour et al., 2003). Thomson and Cunha (1999) reported high levels of FGF10 mRNA in the rat ventral mesenchymal pad, a zone of condensed mesenchymal cells located peripherally within the UGM described previously (Timms et al., 1995). These observations suggest that UGM, the inducer of prostatic epithelial development, is not homogeneous, but instead is regionally specified by morphology (as mesenchymal condensates) (Timms et al., 1995) and by growth factor expression (Thomson and Cunha, 1999). The rat ventral mesenchymal pad is also an inducer of epithelial functionality (specification of secretory protein expression) (Timms et al., 1995; Hayashi et al., 1993), and as a likely regulator of ductal branching patterns (Thomson, 2001). Examination of serial sections of developing human fetal prostates suggest that ductal branching is most intense peripherally near the capsule where α-actin-positive cells are particularly abundant (Fig. 15C), which begs the question as to whether this zone is particularly rich in stromal growth factors? The differentiation of smooth muscle is a highly asymmetric event with α-actin-positive cells initially appear in ventral-lateral UGM near the capsule and subsequently forming a circumferential zone of α-actin-positive smooth muscle near the prostatic capsule (Fig. 15). Future studies should reveal whether this heterogeneity in UGM differentiation is coupled with regional differences in growth factor expression and in induction of ductal branching morphogenesis.

Xenograft studies of human fetal prostates have been carried out previously and support the idea that normal human prostatic development is dependent upon androgens (Yonemura et al., 1995; Sugimura et al., 1988; Saffarini et al., 2013). Such grafts of human fetal prostate

also respond to the adverse effect of exogenous estrogen (Yonemura et al., 1995; Sugimura et al., 1988; Saffarini et al., 2015b; Saffarini et al., 2015a). In the present study we carried out the simple experiment of dividing human fetal prostates into right and left halves, which were grafted into DHT-treated or untreated castrated (androgen-deficient) hosts. In both cases the human fetal prostatic grafts contained solid prostatic buds prior to transplantation. Prostatic ductal morphogenesis, epithelial differentiation and marker expression was enhanced by DHT and retarded as a result of androgen deficiency (untreated castrated hosts) as expected. NKX3.1 3.1 was not detected in the solid prostatic epithelial cords of control (androgen deficient) xenografts, but was expressed in a subset of luminal epithelial cells of canalized ducts observed in DHT-treated prostatic xenografts. Likewise, in grafts of female urethra (analogue of the prostatic urethra) prostatic ductal morphogenesis and epithelial differentiation was induced by DHT which elicited advanced expression of a spectrum of prostate- associated/specific epithelial markers. Significantly, DHT induced the expression of NKX3.1, prostatic specific antigen and prostatic acid phosphatase, thus verifying that ductal structures in xenografts of the DHT-treated human female fetal urethra were indeed prostate. The expression of NKX3.1, prostatic specific antigen and prostatic acid phosphatase in the xenografts was only seen in canalized and not in solid epithelial cords, and thus is dependent upon advanced prostatic epithelial differentiation elicited by androgen. Our observations regarding NKX3.1 differ slightly from that reported in the developing mouse prostate (Bhatia-Gaur et al., 1999) in so far as in the mouse NKX3.1 is expressed in the pre-bud male UGE, in solid prostatic buds and subsequently in canalized prostatic ducts, while in human prostatic development NKX3.1 was only observed in luminized ducts. DHT induction of human PSA (prostate specific antigen) and PAP (prostatic acid phosphatase) in grafts of human female fetal urethra further validates our interpretation that the induced glandular structures are indeed prostatic. Finally, grafts of human female urethra provide the opportunity of examining androgen-induced initiation of human fetal prostatic budding (with induction of NKX3.1, prostatic specific antigen and prostatic acid phosphatase) under controlled experimental conditions. These findings confirm the long established concept that prostatic development is androgen-dependent (Wilson et al., 1981), and emphasize the utility of the xenograft approach for investigation of human prostatic development.

A novel finding that emerged in our xenograft studies is the presence of nerve fibers and neurons in ganglia in grafts of human fetal prostate (Fig. 17F1-F2), which means that neurons can survive the xenografting procedure and provides the opportunity of investigating effects of hormones and other agents on development of innervation of the prostate. An alternate explanation is that the nerves are of host origin. However, the presence of ganglion cells (Fig. 17F1) in the grafts strongly supports the idea of human origin of these cells.

We have shown previously that rat and mouse UGM can induce prostatic development in human fetal and adult urinary bladder epithelium (Cunha et al., 1983; Aboseif et al., 1999). These findings, coupled with the literature on human fetal prostatic xenografts and the findings reported herein, raise the possibility preparing tissue recombinants composed of mutant mouse UGM combined with fetal endodermal epithelium of human origin (from urinary bladder, UGE or female urethra). Such heterospecific tissue recombinants could advance mechanistic studies on human prostatic development.

Acknowledgements:

Abbreviations:

H&E	hematoxylin & eosin
UGS	urogenital sinus
UGE	urogenital sinus epithelium
UGM	urogenital sinus mesenchyme
MDE	Müllerian duct epithelium
AR	androgen receptor
DHT	dihydrotestosterone

References

Aboseif S, El-Sakka A, Young P, and Cunha G (1999) Mesenchymal reprogramming of adult human epithelial differentiation. Differentiation; research in biological diversity 65:113–118. [PubMed: 10550544]

Adams JY, Leav I, Lau KM, Ho SM, and Pflueger SM (2002) Expression of estrogen receptor beta in the fetal, neonatal, and prepubertal human prostate. The Prostate 52:69–81. [PubMed: 11992621]

Allgeier SH, Lin TM, Moore RW, Vezina CM, Abler LL, and Peterson RE (2010) Androgenic regulation of ventral epithelial bud number and pattern in mouse urogenital sinus. Developmental dynamics : an official publication of the American Association of Anatomists 239:373–385. [PubMed: 19941349]

Andersson S, Berman DM, Jenkins EP, and Russell DW (1991) Deletion of steroid 5a-reductase 2 gene in male pseudohermaphroditism. Nature 354:159–161. [PubMed: 1944596]

Andrews GS (1951) The histology of the human foetal and prepubertal prostates. Journal of anatomy 85:44–54. [PubMed: 14814017]

Aumuller G, Holterhus PM, Konrad L, von Rahden B, Hiort O, Esquenet M, and Verhoeven G (1998) Immunohistochemistry and in situ hybridization of the androgen receptor in the developing human prostate. Anatomy and embryology 197:199–208. [PubMed: 9543338]

Besnard V, Wert SE, Hull WM, and Whitsett JA (2004) Immunohistochemical localization of Foxa1 and Foxa2 in mouse embryos and adult tissues. Gene expression patterns : GEP 5:193–208. [PubMed: 15567715]

Bhatia-Gaur R, Donjacour AA, Sciavolino PJ, Kim M, Desai N, Young P, Norton CR, Gridley T, Cardiff RD, Cunha GR, Abate-Shen C, and Shen MM (1999) Roles for Nkx3.1 in prostate development and cancer. Genes & development 13:966–977. [PubMed: 10215624]

Bieberich CJ, Fujita K, He WW, and Jay G (1996) Prostate-specific and androgen- dependent expression of a novel homeobox gene. The Journal of biological chemistry 271:31779–31782. [PubMed: 8943214]

Blake J, and Rosenblum ND (2014) Renal branching morphogenesis: morphogenetic and signaling mechanisms. Semin Cell Dev Biol 36:2–12. [PubMed: 25080023]

Bloch E, Lew M, and Klein M (1971) Studies on the inhibition of fetal androgen formation: testosterone synthesis by fetal and newborn mouse testes in vitro. Endocrinology 88:41–46. [PubMed: 5099584]

Brody H, and Goldman S (1940) Metaplasia of the epithelium of the prostate glands, utricle and urethra of the fetus and newborn infant. Arch. Pathol. 29:494–504.

Clemente CD (ed) (1985) Gray's Anatomy. Lea and Febiger, Philadelphia.

Couse JF, and Korach KS (1999) Estrogen receptor null mice: what have we learned and where will they lead us? Endocrine reviews 20:358–417. [PubMed: 10368776]

Cunha GR, and Baskin L (2016) Use of sub-renal capsule transplantation in developmental biology. Differentiation; research in biological diversity 91:4–9. [PubMed: 26639079]

Cunha GR, Cooke PS, and Kurita T (2004a) Role of stromal-epithelial interactions in hormonal responses. Archives of histology and cytology 67:417–434. [PubMed: 15781983]

Cunha GR, Donjacour AA, Cooke PS, Mee S, Bigsby RM, Higgins SJ, and Sugimura Y (1987) The endocrinology and developmental biology of the prostate. Endocrine Rev. 8:338–362. [PubMed: 3308446]

Cunha GR, Hayward SW, and Wang Y-Z (2002) Role of stroma in carcinogenesis of the prostate. Differentiation; research in biological diversity 60:473–485.

Cunha GR, Ricke W, Thomson A, Marker PC, Risbridger G, Hayward SW, Wang YZ, Donjacour AA, and Kurita T (2004b) Hormonal, cellular, and molecular regulation of normal and neoplastic prostatic development. The Journal of steroid biochemistry and molecular biology 92:221–236. [PubMed: 15663986]

Cunha GR, Sekkingstad M, and Meloy BA (1983) Heterospecific induction of prostatic development in tissue recombinants prepared with mouse, rat, rabbit, and human tissues. Differentiation; research in biological diversity 24:174–180. [PubMed: 6884617]

Darby I, Skalli O, and Gabbiani G (1990) Alpha-smooth muscle actin is transiently expressed by myofibroblasts during experimental wound healing. Laboratory investigation; a journal of technical methods and pathology 63:21–29. [PubMed: 2197503]

Dauge MC, Delmas V, and Mandarim de Lacerda CA (1986) [Development of the human prostate during the first stages of fetal life. Morphometric study]. Bull Assoc Anat (Nancy) 70:5–11.

Dema A, and Tudose N (1998) Immunohistochemical expression of prostate specific antigen (PSA) in benign and malignant tumors of the prostate. Rom J Morphol Embryol 44:93–100. [PubMed: 15678849]

Deslypere JP, Young M, Wilson JD, and McPhaul MJ (1992) Testosterone and 5 alpha-dihydrotestosterone interact differently with the androgen receptor to enhance transcription of the MMTV-CAT reporter gene. Molecular and cellular endocrinology 88:15–22. [PubMed: 1334007]

Diez-Roux G, Banfi S, Sultan M, Geffers L, Anand S, Rozado D, Magen AE, Pagani M, Peluso I, Lin-Marq N, Koch M, Bilio M, Cantiello I, Verde R, De Masi C, Bianchi SA, Cicchini J, Perroud E, Mehmeti S, Dagand E, Schrinner S, Nurnberger A, Schmidt K, Metz K, Zwingmann C, Brieske N, Springer C, Hernandez AM, Herzog S, Grabbe F, Sieverding C, Fischer B, Schrader K, Brockmeyer M, Dettmer S, Helbig C, Alunni V, Battaini MA, Mura C, Henrichsen CN, Garcia-Lopez R, Echevarria D, Puelles E, Garcia-Calero E, Kruse S, Uhr M, Kauck C, Feng G, Milyaev N, Ong CK, Kumar L, Lam M, Semple CA, Gyenesei A, Mundlos S, Radelof U, Lehrach H, Sarmientos P, Reymond A, Davidson DR, Dolle P, Antonarakis SE, Yaspo ML, Martinez S, Baldock RA, Eichele G, and Ballabio A (2011) A high-resolution anatomical atlas of the transcriptome in the mouse embryo. PLoS Biol 9:e1000582. [PubMed: 21267068]

Donjacour AA, and Cunha GR (1988) The effect of androgen deprivation on branching morphogenesis in the mouse prostate. Develop. Biol. 128:1–14. [PubMed: 3384172]

Donjacour AA, Thomson AA, and Cunha GR (2003) FGF-10 plays an essential role in the growth of the fetal prostate. Developmental biology 261:39–54. [PubMed: 12941620]

Drey EA, Kang MS, McFarland W, and Darney PD (2005) Improving the accuracy of fetal foot length to confirm gestational duration. Obstetrics and gynecology 105:773–778. [PubMed: 15802404]

Dupont S, Krust A, Gansmuller A, Dierich A, Chambon P, and Mark M (2000) Effect of single and compound knockouts of estrogen receptors alpha (ERalpha) and beta (ERbeta) on mouse reproductive phenotypes. Development 127:4277–4291. [PubMed: 10976058]

Eddy EM, Washburn TF, Bunch DO, Goulding EH, Gladen BC, Lubahn DB, and Korach KS (1996) Targeted disruption of the estrogen receptor gene in male mice causes alteration of spermatogenesis and infertility. Endocrinology 137:4796–4805. [PubMed: 8895349]

Feldman SC, and Bloch E (1978) Developmental pattern of testosterone synthesis by fetal rat testes in response to luteinizing hormone. Endocrinology 102:999–1007. [PubMed: 744029]

Georgas KM, Armstrong J, Keast JR, Larkins CE, McHugh KM, Southard- Smith EM, Cohn MJ, Batourina E, Dan H, Schneider K, Buehler DP, Wiese CB, Brennan J, Davies JA, Harding SD, Baldock RA, Little MH, Vezina CM, and Mendelsohn C (2015) An illustrated anatomical ontology of the developing mouse lower urogenital tract. Development 142:1893–1908. [PubMed: 25968320]

Glenister TW (1962) The development of the utricle and of the so-called 'middle' or 'median' lobe of the human prostate. Journal of anatomy 96:443–455. [PubMed: 13948442]

Green EL (1966) Biology of the laboratory mouse. JACKSON LABORATORY, http://www.informatics.jax.org/greenbook/frames/frame13.shtml.

Gugliotta P, Sapino A, Macri L, Skalli O, Gabbiani G, and Bussolati G (1988) Specific demonstration of myoepithelial cells by anti-alpha smooth muscle actin antibody. J Histochem Cytochem 36:659–663. [PubMed: 3367051]

Hayashi N, Cunha GR, and Parker M (1993) Permissive and instructive induction of adult rodent prostatic epithelium by heterotypic urogenital sinus mesenchyme. Epithelial Cell Biol. 2:66–78. [PubMed: 8353595]

Hayashi N, Sugimura Y, Kawamura J, Donjacour AA, and Cunha GR (1991) Morphological and functional heterogeneity in the rat prostatic gland. Biol. Reprod. 45:308–321. [PubMed: 1786296]

Hayward SW, Baskin LS, Haughney PC, Cunha AR, Foster BA, Dahiya R, Prins GS, and Cunha GR (1996a) Epithelial development in the rat ventral prostate, anterior prostate and seminal vesicle. Acta anatomica 155:81–93. [PubMed: 8828706]

Hayward SW, Brody JR, and Cunha GR (1996b) An edgewise look at basal cells: Three-dimensional views of the rat prostate, mammary gland and salivary gland. Differentiation; research in biological diversity 60:219–227. [PubMed: 8765052]

Hayward SW, Olumi AF, Haughney PC, Dahiya R, and Cunha GR (1996c) Prostate adenocarcinoma causes dedifferentiation of its surrounding smooth muscle. Proc Am Urol Assn 155:605A.

Hudson DL, Guy AT, Fry P, O'Hare MJ, Watt FM, and Masters JR (2001) Epithelial cell differentiation pathways in the human prostate. Identification of intermediate phenotypes by keratin expression. J Histochem Cytochem 49:271–278. [PubMed: 11156695]

Iber D, and Menshykau D (2013) The control of branching morphogenesis. Open Biol 3:130088. [PubMed: 24004663]

Imperato-McGinley J, Sanchez RS, Spencer JR, Yee B, and Vaughan ED (1992) Comparison of the effects of the 5a-reductase inhibitor finasteride and the antiandrogen flutamide on prostate and genital differentiation: dose-response studies. Endocrinology 131:1149–1156. [PubMed: 1324152]

Joseph DB, Chandrashekar AS, Abler LL, Chu L-F, Thomson JA, Mendelsohn C, and C.M. V (2018) In vivo replacement of damaged bladder urothelium by Wolffian duct epithelial cells. PNAS (In Press).

Keil KP, Abler LL, Laporta J, Altmann HM, Yang B, Jarrard DF, Hernandez LL, and Vezina CM (2014a) Androgen receptor DNA methylation regulates the timing and androgen sensitivity of mouse prostate ductal development. Developmental biology 396:237–245. [PubMed: 25446526]

Keil KP, Abler LL, Mehta V, Altmann HM, Laporta J, Plisch EH, Suresh M, Hernandez LL, and Vezina CM (2014b) DNA methylation of E-cadherin is a priming mechanism for prostate development. Developmental biology 387:142–153. [PubMed: 24503032]

Kellokumpu-Lehtinen P, and Pelliniemi LJ (1988) Hormonal regulation of differentiation of human fetal prostate and Leydig cells in vitro. Folia Histochem Cytobiol 26:113–117. [PubMed: 3197875]

Kellokumpu-Lehtinen P, Santti RS, and Pelliniemi LJ (1981) Development of human fetal prostate in culture. Urol Res 9:89–98. [PubMed: 7233651]

Kellokumpu-Lehtonen P, Santti R, and Pelliniemi LJ (1980) Correlation of early cytodifferentiation of the human fetal prostate and Leydig cells. Anat. Rec. 196:263–273. [PubMed: 7406220]

Krege JH, Hodgin JB, Couse JF, Enmark E, Warner M, Mahler JF, Sar M, Korach KS, Gustafsson JA, and Smithies O (1998) Generation and reproductive phenotypes of mice lacking estrogen receptor

beta. Proceedings of the National Academy of Sciences of the United States of America 95:15677–15682. [PubMed: 9861029]

Kuslak SL, and Marker PC (2007) Fibroblast growth factor receptor signaling through MEK-ERK is required for prostate bud induction. Differentiation; research in biological diversity 75:638–651. [PubMed: 17309601]

Kuslak SL, Thielen JL, and Marker PC (2007) The mouse seminal vesicle shape mutation is allelic with Fgfr2. Development 134:557–565. [PubMed: 17202188]

Lam KW, Li CY, Yam LT, Sun T, Lee G, and Ziesmer S (1989) Improved immunohistochemical detection of prostatic acid phosphatase by a monoclonal antibody. The Prostate 15:13–21. [PubMed: 2477829]

Lee CH, Akin-Olugbade O, and Kirschenbaum A (2011) Overview of prostate anatomy, histology, and pathology. Endocrinology and metabolism clinics of North America 40:565–575, viii-ix. [PubMed: 21889721]

Letellier G, Perez MJ, Yacoub M, Levillain P, Cussenot O, and Fromont G (2007) Epithelial phenotypes in the developing human prostate. J Histochem Cytochem 55:885–890. [PubMed: 17478449]

Levine AC, Wang JP, Ren M, Eliashvili E, Russell DW, and Kirschenbaum A (1996) Immunohistochemical localization of steroid 5 alpha-reductase 2 in the human male fetal reproductive tract and adult prostate. The Journal of clinical endocrinology and metabolism 81:384–389. [PubMed: 8550782]

Li J, Ding Z, Wang Z, Lu J, Maity S, Navone N, Logothetis C, GB. M, and J. K (2011) Androgen regulation of 5a-reductase isoenzymes in prostate cancer: implications for prostate cancer prevention. PloS one 6:1–12.

Li X, Nokkala E, Yan W, Streng T, Saarinen N, Warri A, Huhtaniemi I, Santti R, Makela S, and Poutanen M (2001) Altered structure and function of reproductive organs in transgenic male mice overexpressing human aromatase. Endocrinology 142:2435–2442. [PubMed: 11356692]

Liaw A, Cunha GR, Shen J, Cao M, Liu G, Sinclair A, and Baskin LS (2018) Embryological Development of the Bladder and Ureterovesical Junction. Differentiation; research in biological diversity (This issue).

Lin TM, Rasmussen NT, Moore RW, Albrecht RM, and Peterson RE (2003) Region-specific inhibition of prostatic epithelial bud formation in the urogenital sinus of C57BL/6 mice exposed in utero to 2,3,7,8-tetrachlorodibenzo-p-dioxin. Toxicological sciences : an official journal of the Society of Toxicology 76:171– 181. [PubMed: 12944588]

Lowsley OS (1912) The development of the human prostate gland with reference to the development of other structures at the neck of the urinary bladder. Am. J. Anat. 13:299–349.

Majumder PK, and Kumar VL (1997) Androgen receptor mRNA detection in the human foetal prostate. International urology and nephrology 29:633–635. [PubMed: 9477359]

Marker PC, Donjacour AA, Dahiya R, and Cunha GR (2003) Hormonal, cellular, and molecular control of prostatic development. Developmental biology 253:165– 174. [PubMed: 12645922]

McNeal JE (1978) Origin and evolution of benign prostatic enlargement. Invest. Urol. 15:340–345. [PubMed: 75197]

McNeal JE (1981) The zonal anatomy of the prostate. The Prostate 2:35–49. [PubMed: 7279811]

McNeal JE (1983) The prostate gland: morphology and pathobiology. Monogr. Urology 4:3–37.

McPherson SJ, Wang H, Jones ME, Pedersen J, Iismaa TP, Wreford N, Simpson ER, and Risbridger GP (2001) Elevated androgens and prolactin in aromatase-deficient mice cause enlargement, but not malignancy, of the prostate gland. Endocrinology 142:2458–2467. [PubMed: 11356695]

Mehta V, Schmitz CT, Keil KP, Joshi PS, Abler LL, Lin TM, Taketo MM, Sun X, and Vezina CM (2013) Beta-catenin (CTNNB1) induces Bmp expression in urogenital sinus epithelium and participates in prostatic bud initiation and patterning. Developmental biology 376:125–135. [PubMed: 23396188]

Moore RW, Rudy TA, Lin TM, Ko K, and Peterson RE (2001) Abnormalities of sexual development in male rats with in utero and lactational exposure to the antiandrogenic plasticizer Di(2-ethylhexyl) phthalate. Environmental health perspectives 109:229–237. [PubMed: 11333183]

Nicholson TM, Moses MA, Uchtmann KS, Keil KP, Bjorling DE, Vezina CM, Wood RW, and Ricke WA (2015) Estrogen receptor-alpha is a key mediator and therapeutic target for bladder complications of benign prostatic hyperplasia. The Journal of urology 193:722–729. [PubMed: 25167991]

Nicholson TM, Ricke EA, Marker PC, Miano JM, Mayer RD, Timms BG, vom Saal FS, Wood RW, and Ricke WA (2012) Testosterone and 17beta- estradiol induce glandular prostatic growth, bladder outlet obstruction, and voiding dysfunction in male mice. Endocrinology 153:5556–5565. [PubMed: 22948219]

Ochoa-Espinosa A, and Affolter M (2012) Branching morphogenesis: from cells to organs and back. Cold Spring Harb Perspect Biol 4.

Olumi AF, Grossfeld GD, Hayward SW, Carroll PR, Tlsty TD, and Cunha GR (1999) Carcinoma-associated fibroblasts direct tumor progression of initiated human prostatic epithelium. Cancer Res. 59:5002–5011. [PubMed: 10519415]

Park WY, Miranda B, Lebeche D, Hashimoto G, and Cardoso WV (1998) FGF- 10 is a chemotactic factor for distal epithelial buds during lung development. Developmental biology 201:125–134. [PubMed: 9740653]

Patel VN, Rebustini IT, and Hoffman MP (2006) Salivary gland branching morphogenesis. Differentiation; research in biological diversity 74:349–364. [PubMed: 16916374]

Prins GS, Huang L, Birch L, and Pu Y (2006) The role of estrogens in normal and abnormal development of the prostate gland. Annals of the New York Academy of Sciences 1089:1–13. [PubMed: 17261752]

Radmayr C, Lunacek A, Schwentner C, Oswald J, Klocker H, and Bartsch G (2008) 5-alpha-reductase and the development of the human prostate. Indian journal of urology : IJU : journal of the Urological Society of India 24:309–312. [PubMed: 19468459]

Ricke EA, Williams K, Lee YF, Couto S, Wang Y, Hayward SW, Cunha GR, and Ricke WA (2012) Androgen hormone action in prostatic carcinogenesis: stromal androgen receptors mediate prostate cancer progression, malignant transformation and metastasis. Carcinogenesis 33:1391–1398. [PubMed: 22535887]

Ricke WA, Lee CW, Clapper TR, Schneider AJ, Moore RW, Keil KP, Abler LL, Wynder JL, Lopez Alvarado A, Beaubrun I, Vo J, Bauman TM, Ricke EA, Peterson RE, and Vezina CM (2016) In Utero and Lactational TCDD Exposure Increases Susceptibility to Lower Urinary Tract Dysfunction in Adulthood. Toxicological sciences : an official journal of the Society of Toxicology 150:429–440. [PubMed: 26865671]

Ricke WA, McPherson SJ, Bianco JJ, Cunha GR, Wang Y, and Risbridger GP (2008) Prostatic hormonal carcinogenesis is mediated by in situ estrogen production and estrogen receptor alpha signaling. FASEB journal : official publication of the Federation of American Societies for Experimental Biology 22:1512–1520. [PubMed: 18055862]

Robboy SJ, Kurita T, Baskin L, and Cunha GR (2017) New insights insights into human female reproductive tract development. Differentiation; research in biological diversity 97:9–22. [PubMed: 28918284]

Rodriguez E, Jr., Weiss DA, Ferretti M, Wang H, Menshenia J, Risbridger G, Handelsman D, Cunha G, and Baskin L (2012) Specific morphogenetic events in mouse external genitalia sex differentiation are responsive/dependent upon androgens and/or estrogens. Differentiation; research in biological diversity 84:269–279. [PubMed: 22925506]

Russell DW, and Wilson JD (1994) Steroid 5 alpha-reductase: two genes/two enzymes. Annu Rev Biochem 63:25–61. [PubMed: 7979239]

Russell WE, Dempsey PJ, Sitaric S, Peck AJ, and Coffey RJ (1993) Transforming growth factor-a (TGFa) concentrations increase in regenerating rat liver: Evidence for a delayed accumulation of mature TGFa. Encocrinology 133:1731–1738.

Saffarini CM, McDonnell EV, Amin A, Spade DJ, Huse SM, Kostadinov S, Hall SJ, and Boekelheide K (2013) Maturation of the developing human fetal prostate in a rodent xenograft model. The Prostate 73:1761–1775. [PubMed: 24038131]

Saffarini CM, McDonnell-Clark EV, Amin A, and Boekelheide K (2015a) A human fetal prostate xenograft model of developmental estrogenization. International journal of toxicology 34:119–128. [PubMed: 25633637]

Saffarini CM, McDonnell-Clark EV, Amin A, Huse SM, and Boekelheide K (2015b) Developmental exposure to estrogen alters differentiation and epigenetic programming in a human fetal prostate xenograft model. PloS one 10:e0122290. [PubMed: 25799167]

Sciavolino PJ, Abrams EW, Yang L, Austenberg LP, Shen MM, and Abate- Shen C (1997) Tissue-specific expression of murine Nkx3.1 in the male urogenital system. Developmental dynamics : an official publication of the American Association of Anatomists 209:127–138. [PubMed: 9142502]

Sebe P, Schwentner C, Oswald J, Radmayr C, Bartsch G, and Fritsch H (2005) Fetal development of striated and smooth muscle sphincters of the male urethra from a common primordium and modifications due to the development of the prostate: an anatomic and histologic study. The Prostate 62:388–393. [PubMed: 15389795]

Shapiro E, Huang H, Masch RJ, McFadden DE, Wilson EL, and Wu XR (2005) Immunolocalization of estrogen receptor alpha and beta in human fetal prostate. The Journal of urology 174:2051–2053. [PubMed: 16217392]

Shapiro E, Huang H, McFadden DE, Masch RJ, Ng E, Lepor H, and Wu XR (2004) The prostatic utricle is not a Mullerian duct remnant: immunohistochemical evidence for a distinct urogenital sinus origin. The Journal of urology 172:1753–1756; discussion 1756. [PubMed: 15371806]

Shappell SB, Thomas GV, Roberts RL, Herbert R, Ittmann MM, Rubin MA, Humphrey PA, Sundberg JP, Rozengurt N, Barrios R, Ward JM, and Cardiff RD (2004) Prostate pathology of genetically engineered mice: definitions and classification. The consensus report from the Bar Harbor meeting of the Mouse Models of Human Cancer Consortium Prostate Pathology Committee. Cancer research 64:2270–2305. [PubMed: 15026373]

Shen J, Cunha GR, Sinclair A, Cao M, Isaacson D, and Baskin L (2018a) Macroscopic whole-mounts of the developing human fetal urogenital-genital tract: indifferent stage to male and female differentiation. Differentiation; research in biological diversity (This issue).

Shen J, Isaacson D, Cao M, Sinclair A, Cunha GR, and Baskin L (2018b) Immunohistochemical expression analysis of the human fetal lower urogenital tract. Differentiation; research in biological diversity (This issue).

Shen J, Liu B, Sinclair A, Cunha G, Baskin LS, and Choudhry S (2015) Expression Analysis of DGKK during External Genitalia Formation. The Journal of urology 194:1728–1736. [PubMed: 26162297]

Singh M, Jha R, Melamed J, Shapiro E, Hayward SW, and Lee P (2014) Stromal androgen receptor in prostate development and cancer. The American journal of pathology 184:2598–2607. [PubMed: 25088980]

Smith B (2016) The Multi-Dimensional Human Embryo University of Michigan, Ann Arbor, MI.

Staack A, Donjacour AA, Brody J, Cunha GR, and Carroll P (2003) Mouse urogenital development: a practical approach. Differentiation; research in biological diversity 71:402–413. [PubMed: 12969333]

Sternlicht MD, Kouros-Mehr H, Lu P, and Werb Z (2006) Hormonal and local control of mammary branching morphogenesis. Differentiation; research in biological diversity 74:365–381. [PubMed: 16916375]

Streeter GL (1951) Developmental horizons in human embryos. Age groups XI to XXIII. Carnegie Institution of Washington, Washington DC.

Sugimura Y, Cunha GR, and Bigsby RM (1986a) Androgenic induction of deoxyribonucleic acid synthesis in prostatic glands induced in the urothelium of testicular feminized (Tfm/y) mice. The Prostate 9:217–225. [PubMed: 2946028]

Sugimura Y, Cunha GR, and Donjacour AA (1986b) Morphogenesis of ductal networks in the mouse prostate. Biol. Reprod. 34:961–971. [PubMed: 3730488]

Sugimura Y, Cunha GR, and Donjacour AA (1986c) Prostatic glandular architecture: Wholemount analysis of morphogenesis and androgen dependency In: Rodgers CH, Coffey DS, Cunha GR, Grayhack JT, Hinman F, and Horton R (eds) Benign Prostatic Hyperplasia. U.S. Govt. Printing Office, Washington, D.C., pp. 55–72.

Sugimura Y, Cunha GR, Donjacour AA, Bigsby RM, and Brody JR (1986d) Whole-mount autoradiography study of DNA synthetic activity during postnatal development and androgen-induced regeneration in the mouse prostate. Biol. Reprod. 34:985–995. [PubMed: 3730490]

Sugimura Y, Cunha GR, Yonemura CU, and Kawamura J (1988) Temporal and spatial factors in diethylstilbestrol-induced squamous metaplasia of the developing human prostate. Hum Pathol 19:133–139. [PubMed: 3343029]

Sugimura Y, Foster BA, Hom YK, Lipschutz JH, Rubin JS, Finch PW, Aaronson SA, Hayashi N, Kawamura J, and Cunha GR (1996) Keratinocyte growth factor (KGF) can replace testosterone in the ductal branching morphogenesis of the rat ventral prostate. The International journal of developmental biology 40:941–951. [PubMed: 8946242]

Szczyrba J, Niesen A, Wagner M, and Wandernoth PM (2017) Neuroendocrine cells of the prostate derive from the neural crest. J. Biological Chemistry 292:2021–2031.

Taylor JA, Richter CA, Suzuki A, Watanabe H, Iguchi T, Coser KR, Shioda T, and vom Saal FS (2012) Dose-related estrogen effects on gene expression in fetal mouse prostate mesenchymal cells. PloS one 7:e48311. [PubMed: 23144751]

Taylor JA, Vom Saal FS, Welshons WV, Drury B, Rottinghaus G, Hunt PA, Toutain PL, Laffont CM, and VandeVoort CA (2011) Similarity of bisphenol A pharmacokinetics in rhesus monkeys and mice: relevance for human exposure. Environmental health perspectives 119:422–430. [PubMed: 20855240]

Thomson AA (2001) Role of androgens and fibroblast growth factors in prostatic development. Reproduction 121:187–195. [PubMed: 11226043]

Thomson AA, and Cunha GR (1999) Prostatic growth and development are regulated by FGF10. Development 126:3693–3701. [PubMed: 10409514]

Timms B, Lee C, Aumuller G, and Seitz J (1995) Instructive induction of prostate growth and differentiation by a defined urogenital sinus mesenchyme. Microscopy Res. and Technique 30:319–332.

Timms BG (1997) Anatomical perspectives of prostate development In: N'az RK (ed) Prostate: Basic and Clinical Aspects. CRC Press, Boca Raton, pp. 39–51.

Timms BG (2008) Prostate development: a historical perspective. Differentiation; research in biological diversity 76:565–577. [PubMed: 18462432]

Timms BG, and Hofkamp LE (2011) Prostate development and growth in benign prostatic hyperplasia. Differentiation; research in biological diversity 82:173–183. [PubMed: 21939815]

Timms BG, Howdeshell KL, Barton L, Bradley S, Richter CA, and vom Saal FS (2005) Estrogenic chemicals in plastic and oral contraceptives disrupt development of the fetal mouse prostate and urethra. Proceedings of the National Academy of Sciences of the United States of America 102:7014–7019. [PubMed: 15867144]

Timms BG, Mohs TJ, and DiDio JA (1994) Ductal budding and branching patterns in the developing prostate. J. Urol. 151:1427–1432. [PubMed: 8158800]

Timms BG, Petersen SL, and vom Saal FS (1999) Prostate gland growth during development is stimulated in both male and female rat fetuses by intrauterine proximity to female fetuses. The Journal of urology 161:1694–1701. [PubMed: 10210442]

Uemura M, Tamura K, Chung S, Honma S, Okuyama A, Nakamura Y, and Nakagawa H (2008) Novel 5 alpha-steroid reductase (SRD5A3, type-3) is overexpressed in hormone-refractory prostate cancer. Cancer Sci. 99:81–86. [PubMed: 17986282]

Vives V, Alonso G, Solal AC, Joubert D, and Legraverend C (2003) Visualization of SlOOB-positive neurons and glia in the central nervous system of EGFP transgenic mice. J Comp Neurol 457:404–419. [PubMed: 12561079]

vom Saal FS, Timms BG, Montano MM, Palanza P, Thayer KA, Nagel SC, Dhar MD, Ganjam VK, Parmigiani S, and Welshons WV (1997) Prostate enlargement in mice due to fetal exposure to low doses of estradiol or diethylstilbestrol and opposite effects at high doses. Proceedings of the National Academy of Sciences of the United States of America 94:2056–2061. [PubMed: 9050904]

Wang S, Sekiguchi R, Daley WP, and Yamada KM (2017) Patterned cell and matrix dynamics in branching morphogenesis. J Cell Biol 216:559–570. [PubMed: 28174204]

Wang Y, Hayward S, Cao M, Thayer K, and Cunha G (2001) Cell differentiation lineage in the prostate. Differentiation; research in biological diversity 68:270–279. [PubMed: 11776479]

Weaver M, Dunn NR, and Hogan BL (2000) Bmp4 and Fgf10 play opposing roles during lung bud morphogenesis. Development 127:2695–2704. [PubMed: 10821767]

Weniger J-P, and Zeis A (1972) Sur la secretion precoce de testosterone parle testicule embryonnaire de souris. C. R. Acad. Sci. Paris 275:1431–1433.

Wernert N, Seitz G, and Achtstatter T (1987) Immunohistochemical investigation of different cytokeratins and vimentin in the prostate from the fetal period up to adulthood and in prostate carcinoma. Path. Res. Pract. 182:617–626. [PubMed: 2446293]

Wilson J, George F, and Griffin J (1981) The hormonal control of sexual development. Science 211:1278–1284. [PubMed: 7010602]

Xia T, Blackburn WR, and Gardner WA, Jr. (1990) Fetal prostate growth and development. Pediatr Pathol 10:527–537. [PubMed: 1695372]

Xue Y, van der Laak J, Smedts F, Schoots C, Verhofstad A, de la Rosette J, and Schalken J (2000) Neuroendocrine cells during human prostate development: does neuroendocrine cell density remain constant during fetal as well as postnatal life? The Prostate 42:116–123. [PubMed: 10617868]

Yamada G, Satoh Y, Baskin LS, and Cunha GR (2003) Cellular and molecular mechanisms of development of the external genitalia. Differentiation; research in biological diversity 71:445–460. [PubMed: 14641326]

Yonemura CY, Cunha GR, Sugimura Y, and Mee SL (1995) Temporal and spatial factors in diethylstilbestrol-induced squamous metaplasia in the developing human prostate. II. Persistent changes after removal of diethylstilbestrol. Acta anatomica 153:1–11. [PubMed: 8560954]

Zhu G, Zhau HE, He H, Zhang L, Shehata B, Wang X, Cerwinka WH, Elmore J, and He D (2007) Sonic and desert hedgehog signaling in human fetal prostate development. The Prostate 67:674–684. [PubMed: 17342747]

Zondek LH, and Zondek T (1979) Effect of hormones on the human fetal prostate. Contrib Gynecol Obstet 5:145–158. [PubMed: 365451]

Zondek LH, and Zondek T (1980) Observations on the prostatic utricle in the fetus and infant. Acta Paediatr Scand 69:257–258. [PubMed: 7189318]
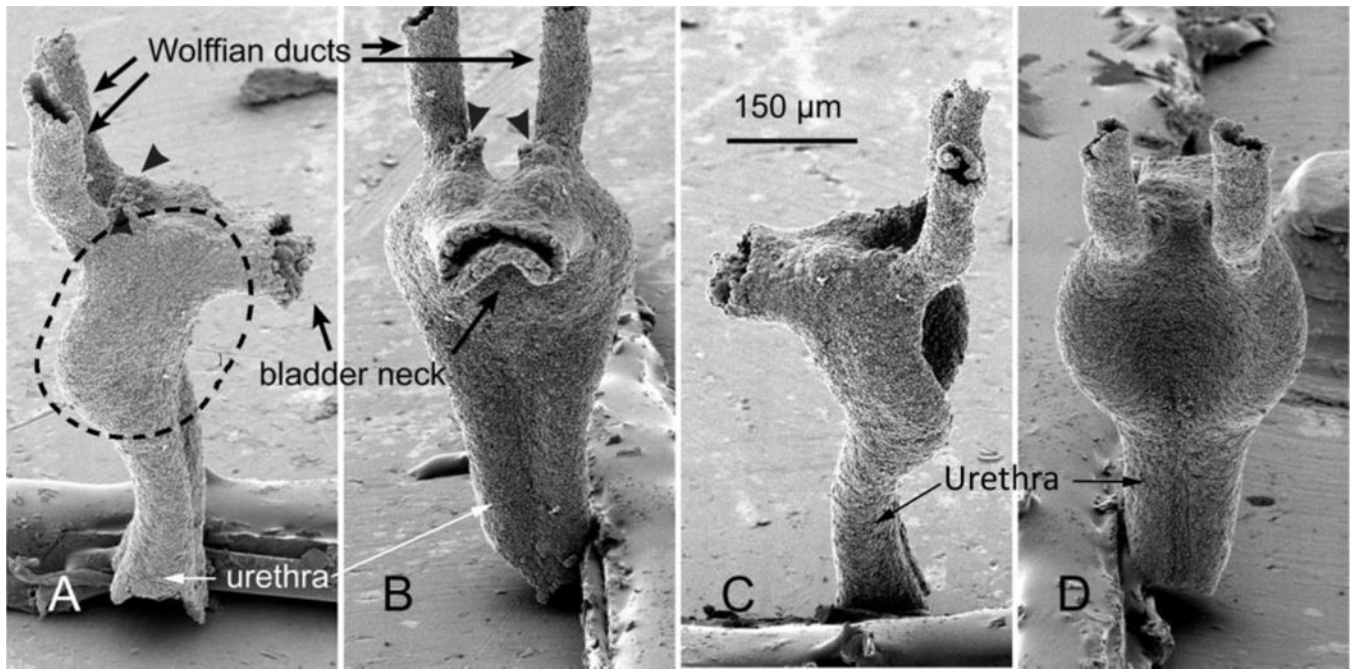
Figure 1.
UGS epithelium from a fetal mouse on gestation day 15 after removal of the mesenchyme. Images were taken by scanning electron microscopy (SEM) at successive 90° rotations of the sample, starting with a lateral view (A). Dotted line in (A) indicates that portion of the UGS from which prostatic buds will emerge. Arrowheads show where the Mullerian ducts entered the UGS epithelium. From Lin et al (2003) with permission.
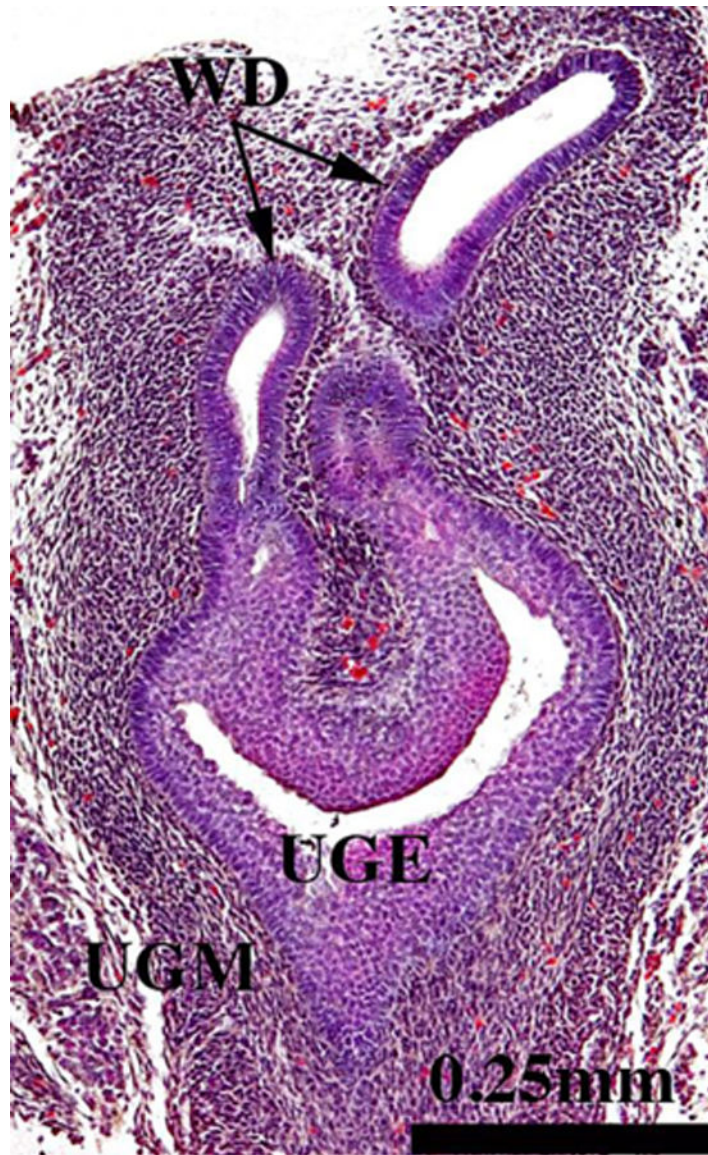
Figure 2.
Section of the urogenital sinus of a 16-day mouse embryo (pre-bud stage) showing urogenital sinus epithelium (UGE), dense urogenital sinus mesenchyme (UGM) and Wolffian ducts (WD). Prostatic buds have not yet developed.
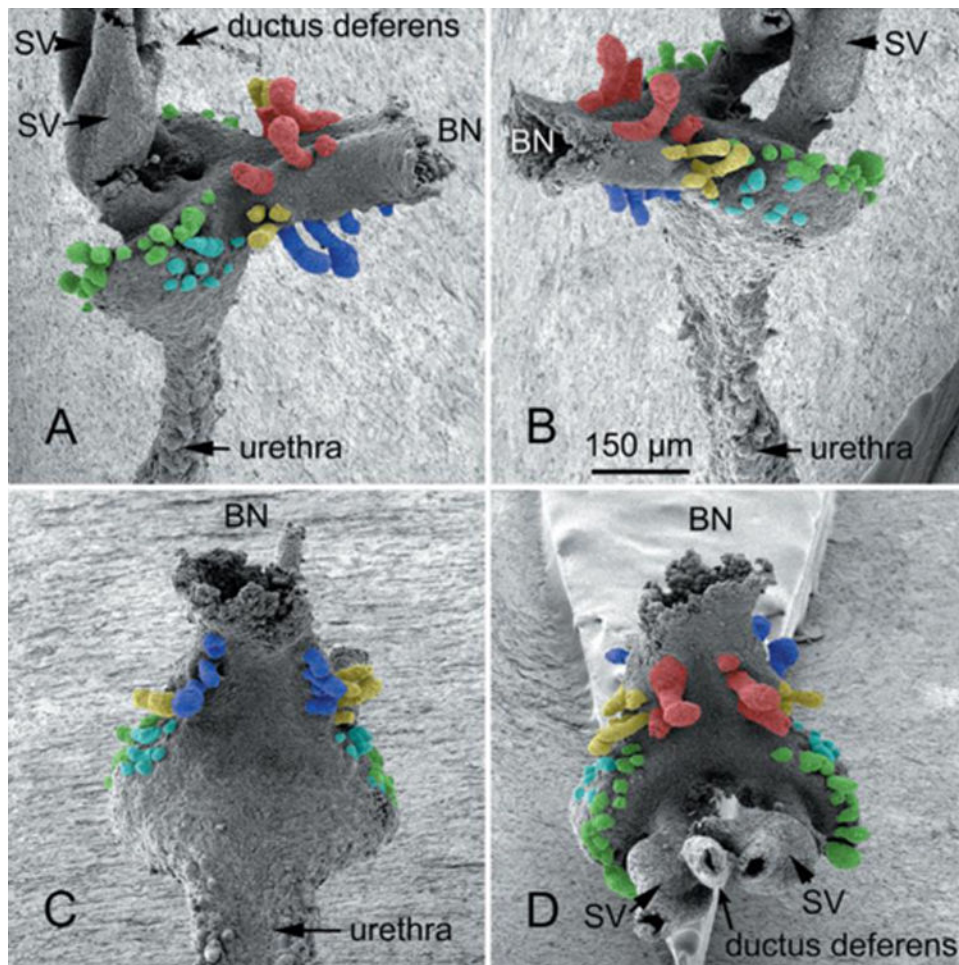
Figure 3.
UGS epithelium from a wild-type fetal mouse on gestation day 18 after removal of the mesenchyme. Two lateral views (A and B), a view of ventral buds (C), and a view of anterior and dorsal buds (D) taken by SEM. Ventral buds (blue), dorsal buds (green), lateral buds (yellow), anterior buds (red), bladder neck (BN), and seminal vesicles (SV) are shown. Prostatic epithelial buds on the lateral surfaces of the UGS that are difficult to classify as either lateral or dorsal buds are tinted blue-green. From Lin et al (2003) with permission. Scale bar in (B) applies to all images.
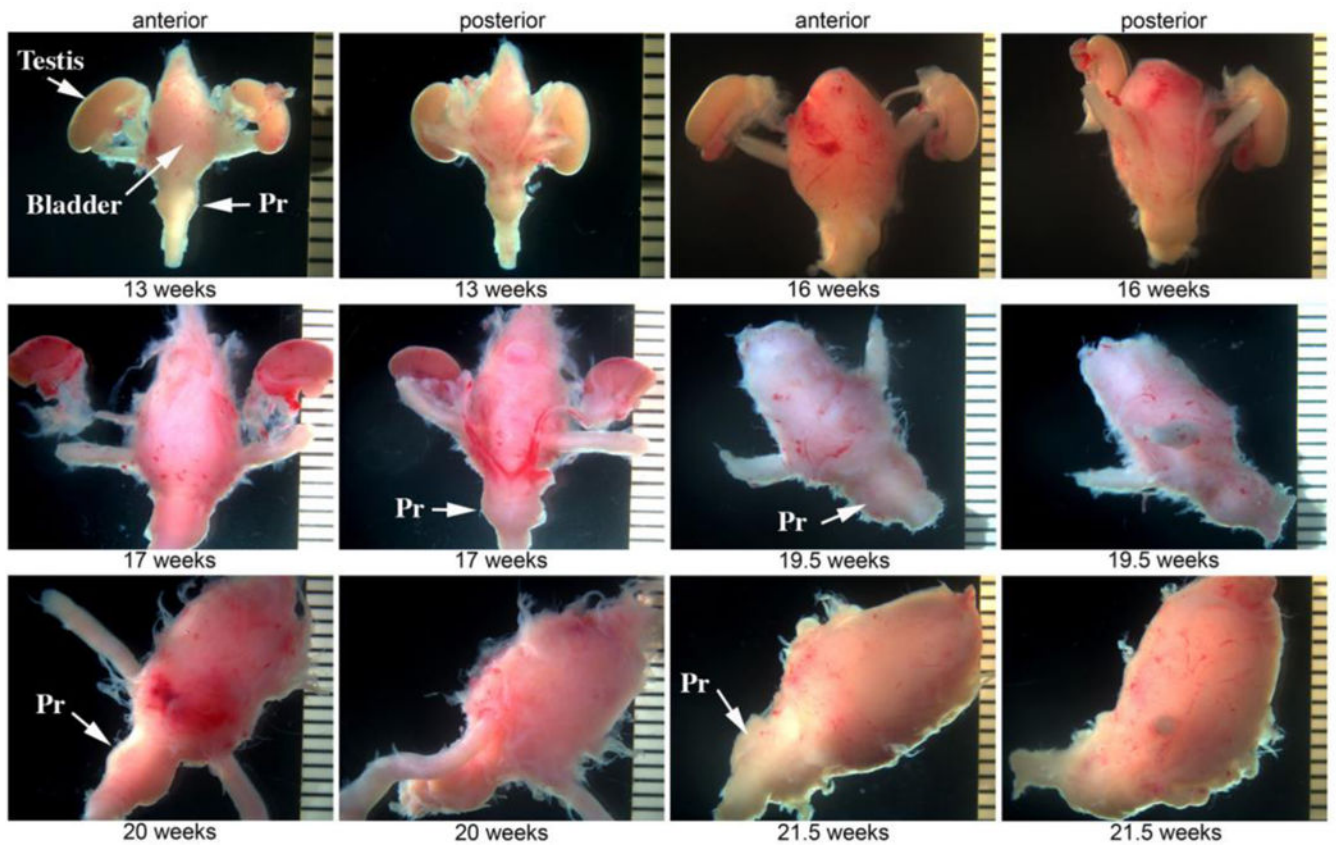
Figure 4.
Wholemount images of human fetal prostates and bladders from 13 to 21 weeks. The prostate is the distinct bulge below the bladder (arrows). Pr=prostate.
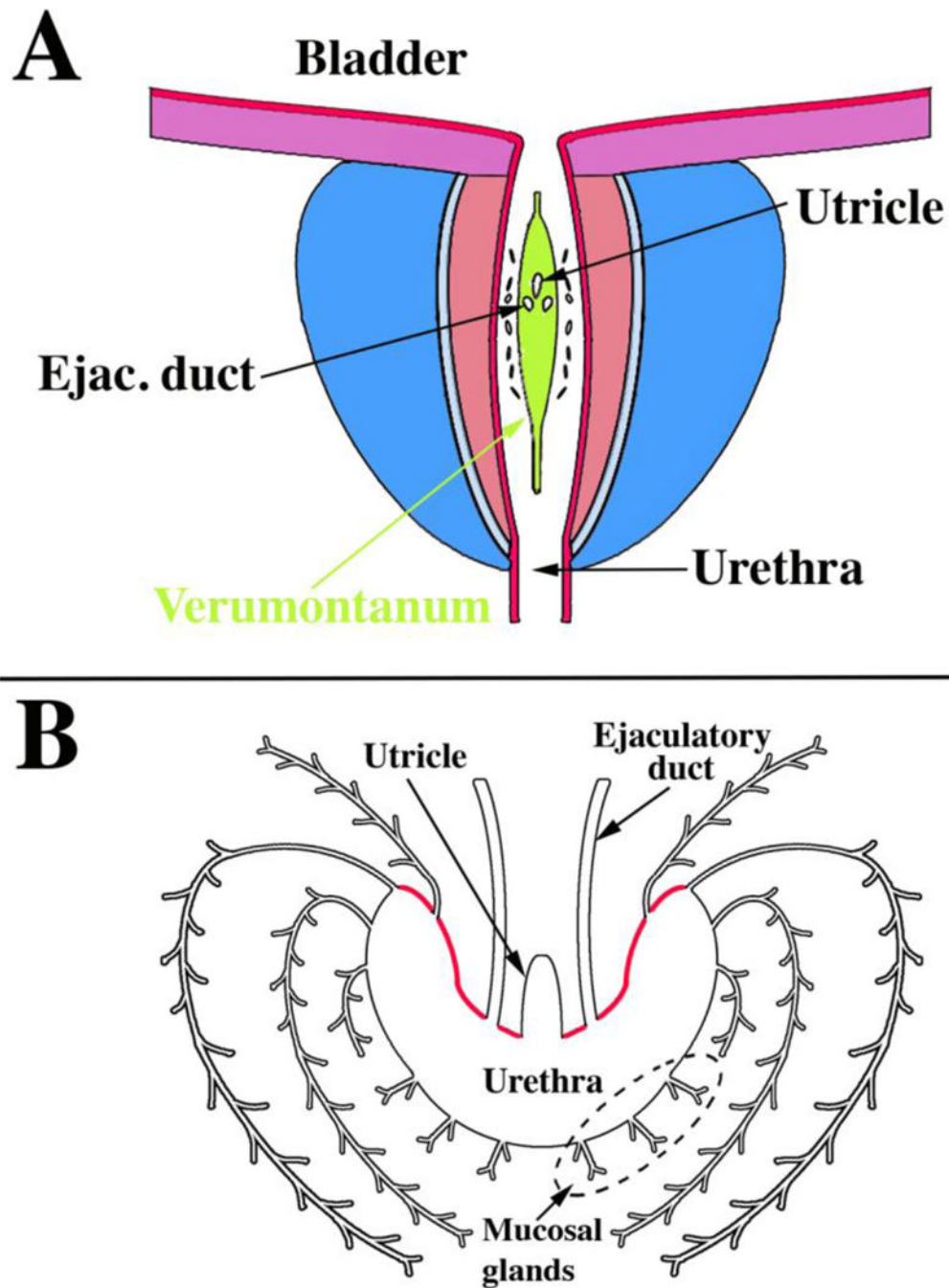
Figure 5.
Drawings of adult human prostate. (A) Anterior wall of the urethra has been removed to visualize the verumontanum (green) as well as the posterior and lateral walls of the prostatic urethra. Note the distribution of openings of the prostatic ducts in the sulci (urethral recesses or furrows) lateral to the verumontanum as described previously (Timms, 1997). (B) Drawing of a transverse section through the verumontanum (highlighted in red) of an adult human prostate showing the prostatic utricle and ejaculatory ducts joining the prostatic urethra. The prostatic ducts emerge from the urethra in the recesses lateral to the

verumontanum. Mucosal glands emerge from the ventral aspect of the urethra. Ejac. duct= ejaculatory duct.
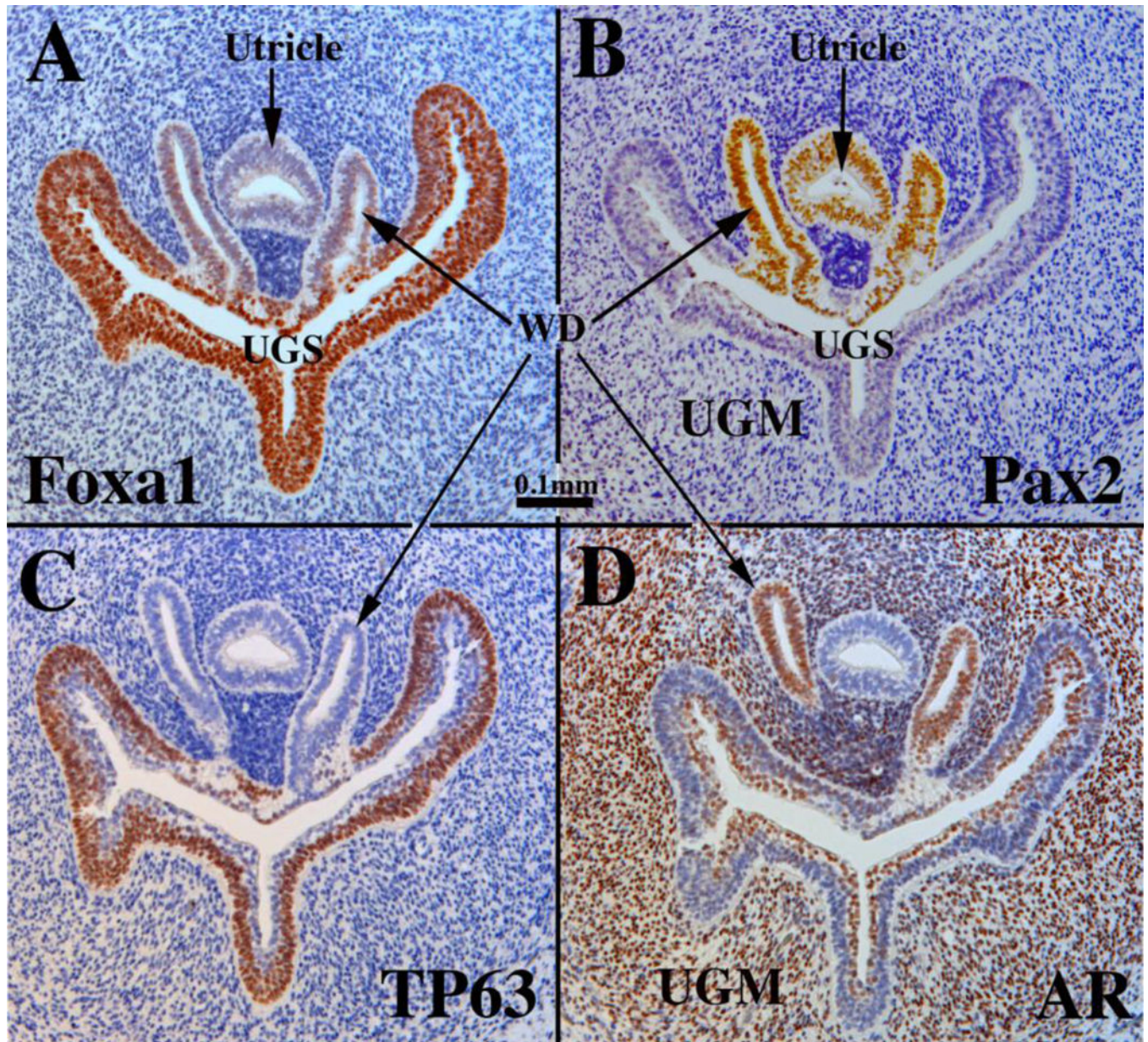
Figure 6.
Sections of a pre-bud 9-week human fetal urogenital sinus (UGS) in the region of the verumontanum, which is a dorsal prominence projecting into the UGS. The Wolffian ducts (WD) flank the Mullerian-derived prostatic utricle, which opens into the UGS at/near the apex of the verumontanum. Sections are immunostained for Foxa1 (A), Pax2 (B), TP63 (C), and androgen receptor (AR) (D) as indicated. Scale bar applies to all images.
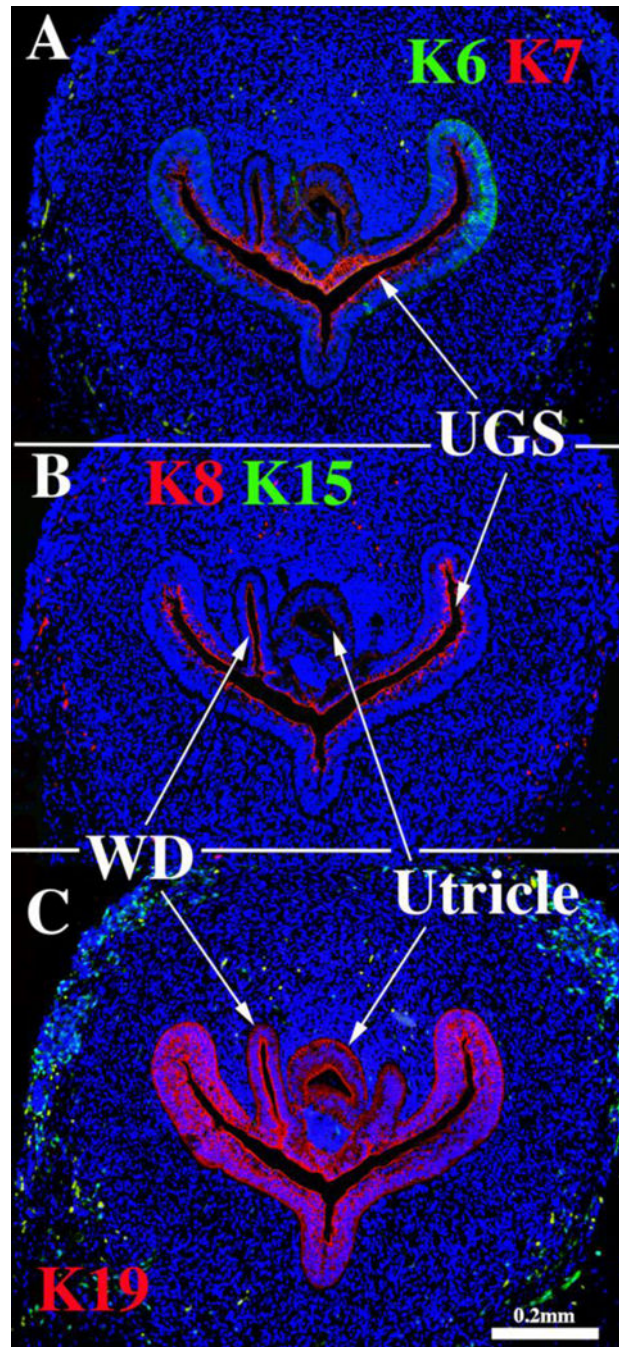
Figure 7.
Sections through the verumontanum of a 9-week pre-bud UGS immunostained for keratins 6 & 7 (A), keratins 8 & 15 (B) and keratin 19 (C). WD= Wolffian duct, UGS= urogenital sinus.
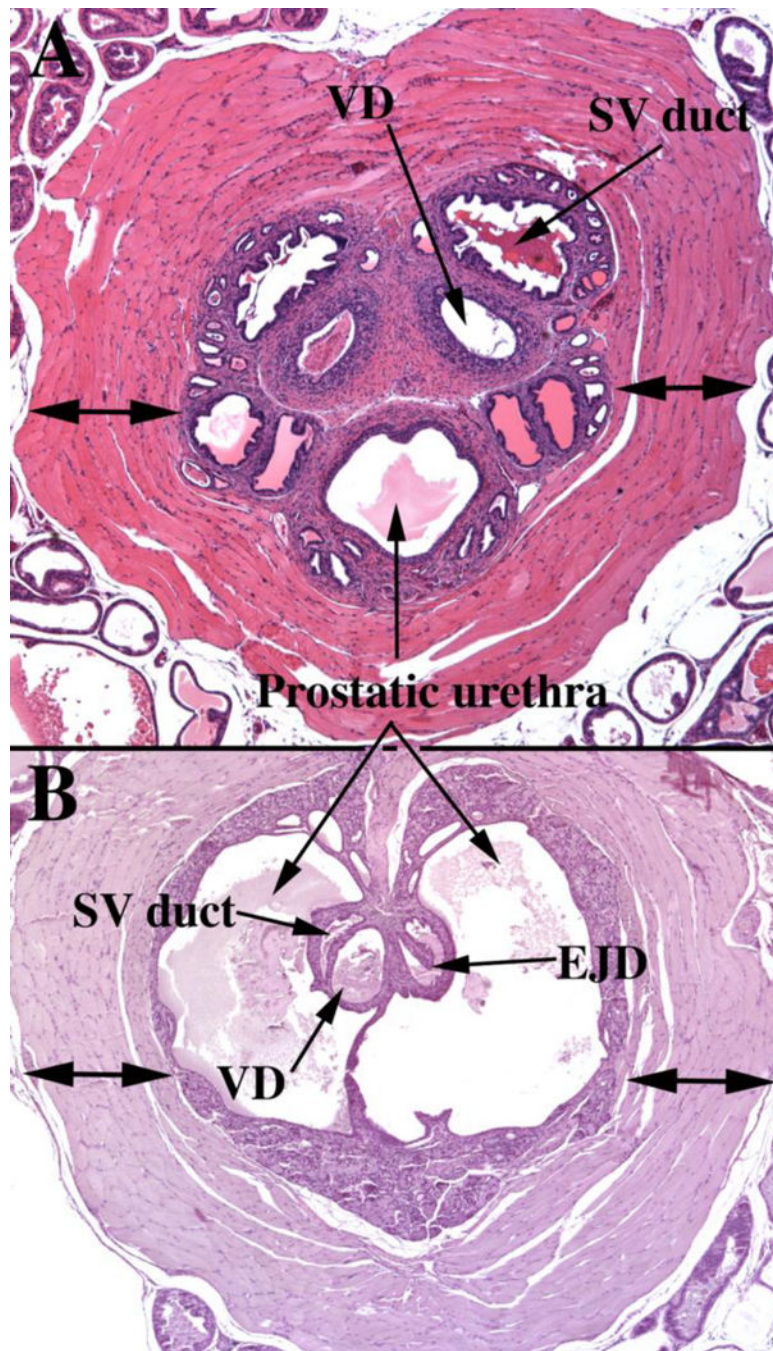
Figure 8.
(A) Section of the adult mouse prostate just cranial to the verumontanum. Dorsal to the prostatic urethra are the paired ducts of the seminal vesicles (SV duct) and the vas deferens (VD). Note the thick rhabdosphincter (double-headed arrows) surrounding the central structures. (B) A section of the adult mouse prostate at the level of the verumontanum, which projects into the prostatic urethra and at this level is tethered dorsally and ventrally to the wall of the prostatic urethra. The left side of the verumontanum displays the crescent-shaped seminal vesicle duct (SV duct) dorsal to the vas deferens (VD). On the right side of

the verumontanum, these two ducts have joined to form an ejaculatory duct (EJD). Surrounding the prostatic urethra and internal to the rhabdosphincter is a circumferential layer of peri-urethra glands (not labeled).
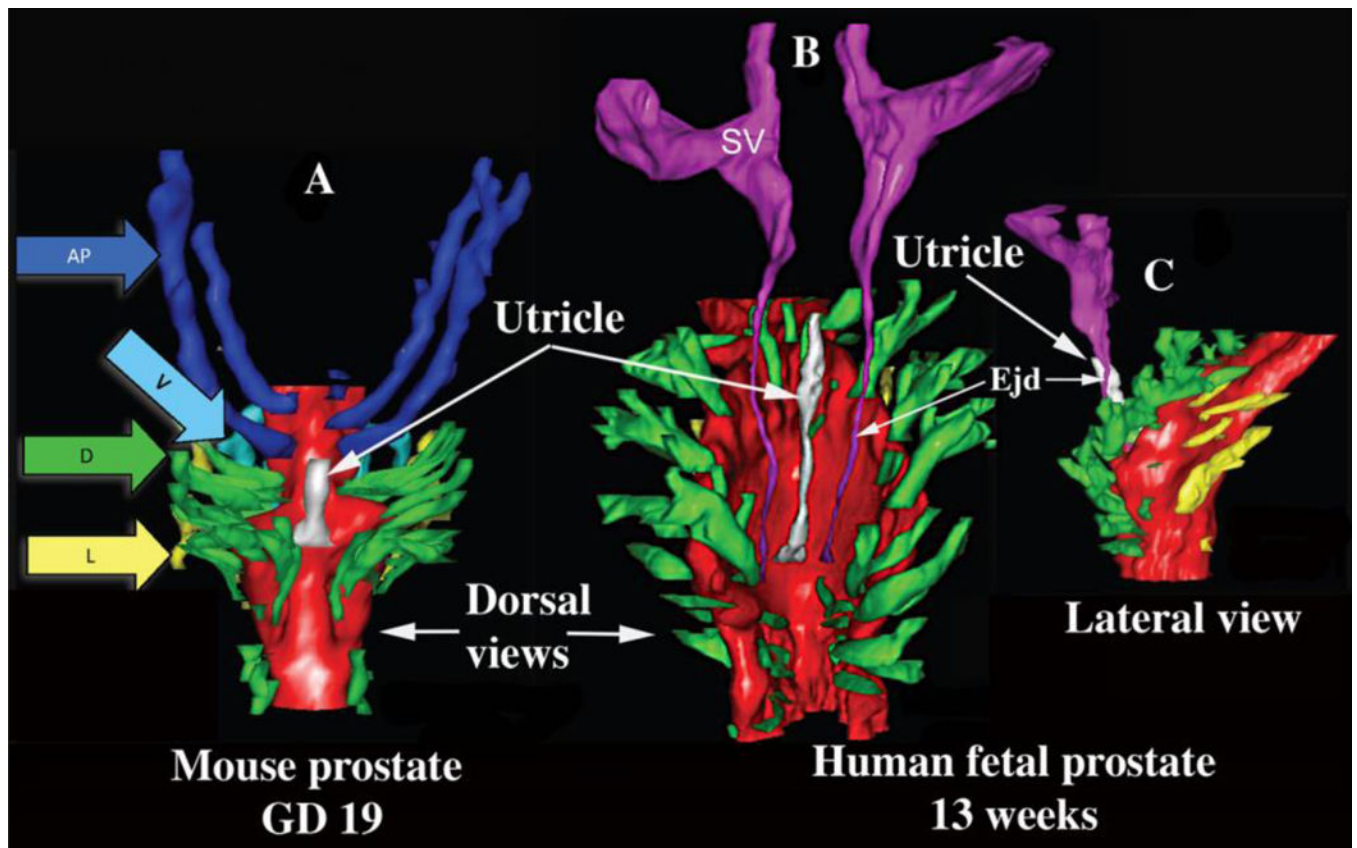
Figure 9.
Three-dimensional reconstruction of mouse and human prostates. (A) Dorsal view of a newborn mouse urogenital sinus reconstruction showing the dorsal prostatic outgrowths (in green, arrow D) situated lateral to the prostatic utricle (white). The seminal vesicles (SV) and ejaculatory ducts have been removed from this reconstruction to clearly illustrate that the most cranial ducts from the elongated and paired anterior prostates (dark blue, AP), also known as the coagulating glands which lie adjacent to the mouse seminal vesicles. Also shown are a few of the lateral (yellow, arrow L) and ventral (light blue, arrow V) prostatic ducts. The prostatic utricle is the midline structure in white. (B) Dorsal view of a 13-week male human fetal prostate showing a similar paired pattern of prostatic ductal outgrowths from the UGS. The most cranial dorsal prostate outgrowths correspond to the equivalent anatomical location of the mouse coagulating glands. At these stages of ductal growth, the mouse and human prostate budding patterns demonstrate striking similarities. The human prostatic utricle is the midline structure in white, and also shown are the seminal vesicles (SV). (C) Lateral view of the same human UGS. Modified from (Timms, 2008) and (Timms and Hofkamp, 2011).
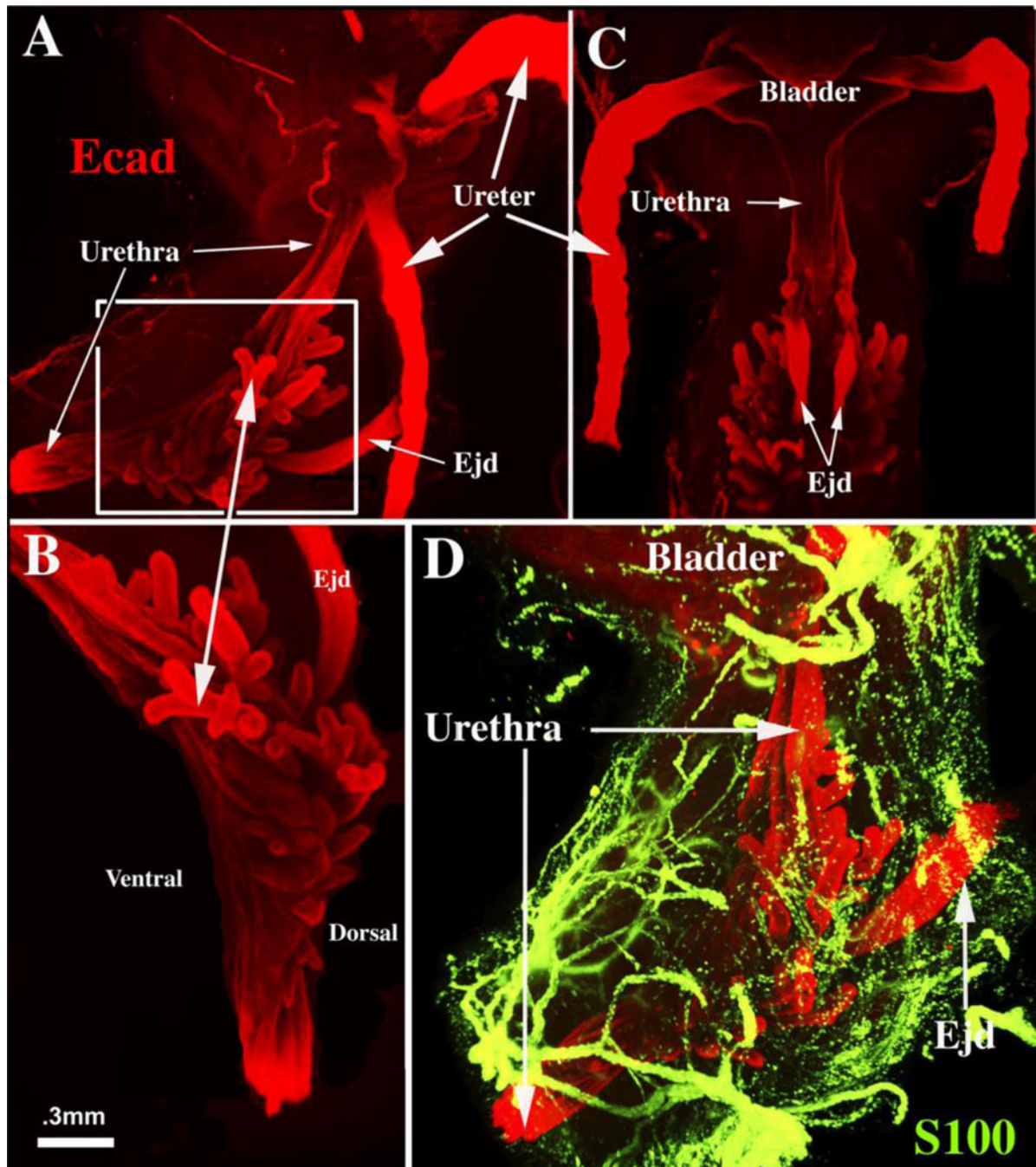
Figure 10.
Light sheet™ three-dimensional reconstruction of a 12-week human fetal prostate immunostained for E-cadherin (red, A-C) to display epithelium and S100 (D, green) to display neurons. Lateral views (A, B & D) and dorsal view (C). Boxed area in (A) is enlarged in (B) to show elongating and branching prostatic buds. (D) Shows the rich network of ganglion cells and neuronal processes that are associated with the developing human prostate. Ejd= ejaculatory ducts.
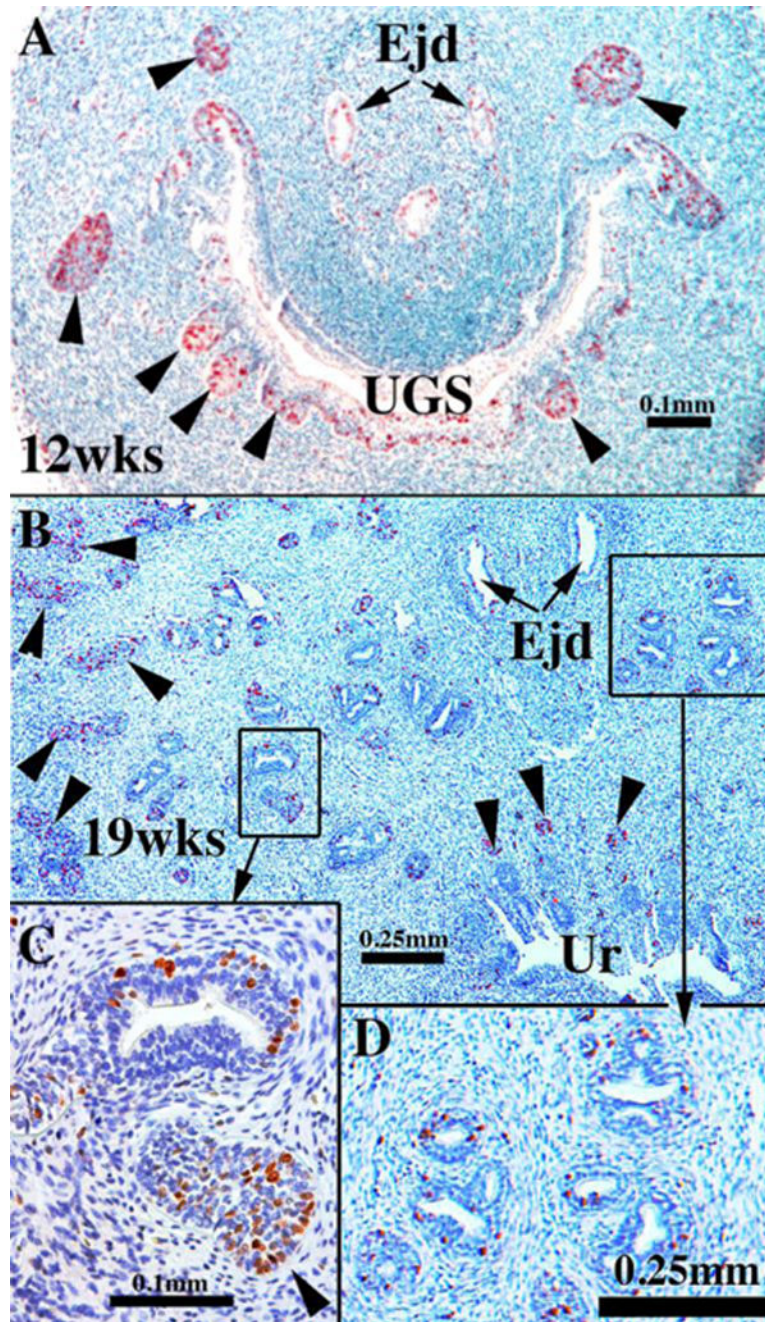
Figure 11.
Sections of human fetal prostates stained for Ki67 at the ages indicated showing solid prostatic epithelial buds/cords heavily labeled with Ki67 (arrowheads) and reduced Ki67 labeling in luminized ducts and in the urethra (Ur). Ejd= Ejaculatory ducts, Ur= Urethra, UGS= urogenital sinus.
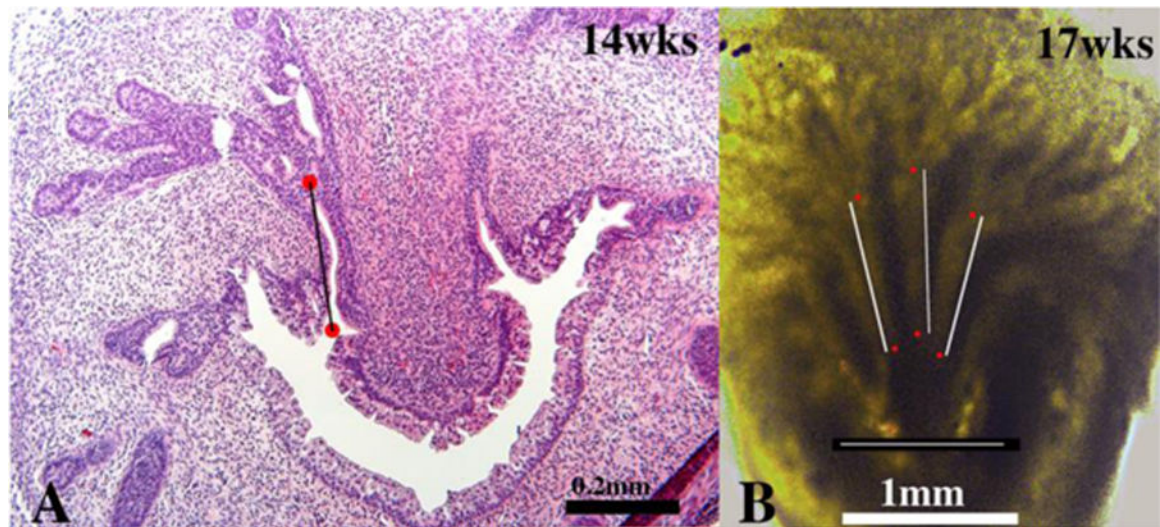
Figure 12.
(A) Section of human fetal prostate at 14 weeks of gestation. The red dots indicate the proximal origin of a prostatic duct and the first branch point, respectively. The distance between these two points is ~250μm. (B) A thick (0.5mm) coronal section of a 17-week human fetal prostate photographed with transmitted light. Red dots are placed on 3 prostatic ducts depicting ductal length to the first branch point. In all three cases the distance is ~1000μιм. The thin white line above the scale bar in (B) is ~1000μιм.
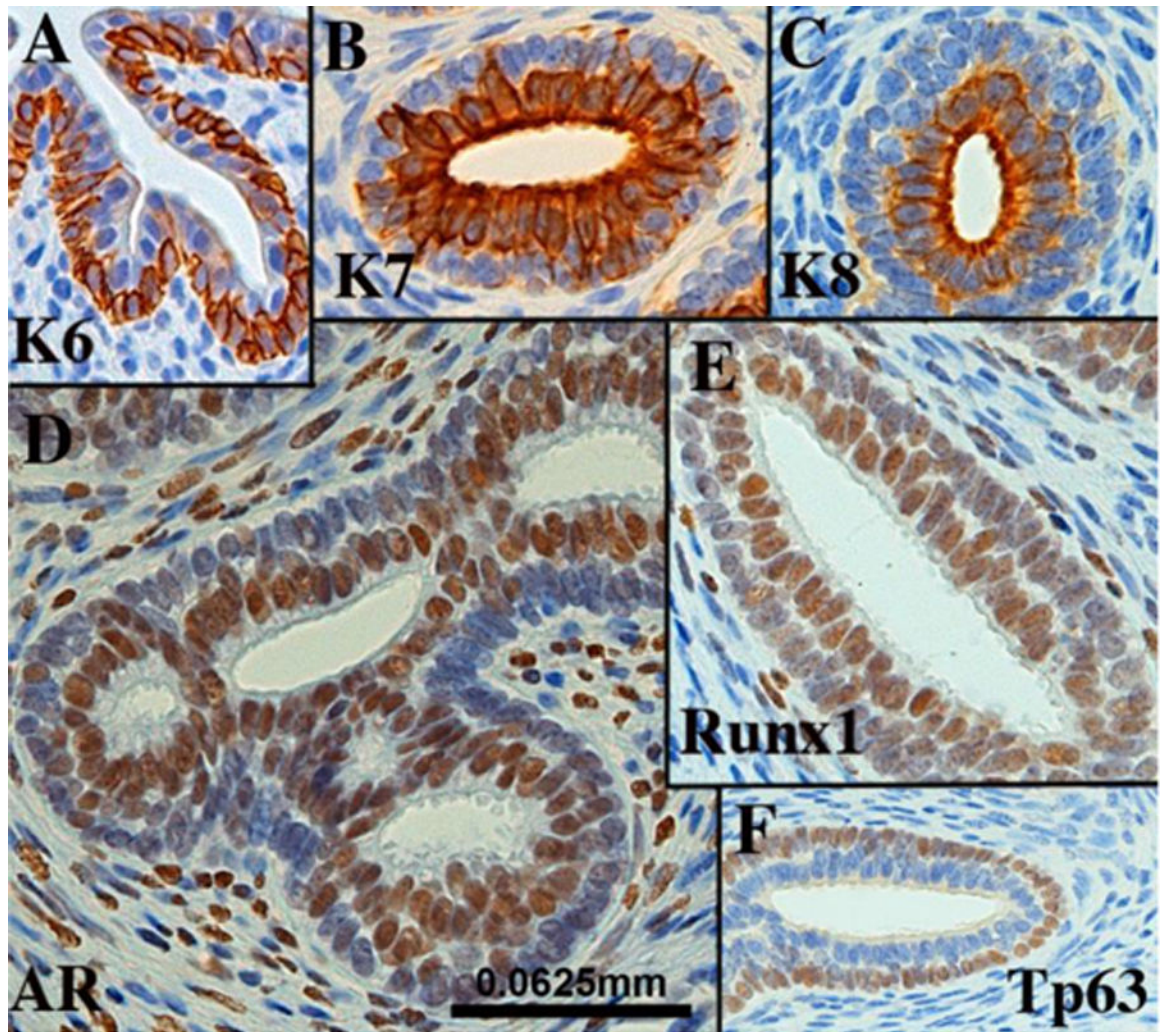
Figure 13.
Sections of canalized human fetal prostatic ducts from 15- to 19-week fetuses exhibiting advanced differentiation immunostained as indicated. Scale bar applies to all images.
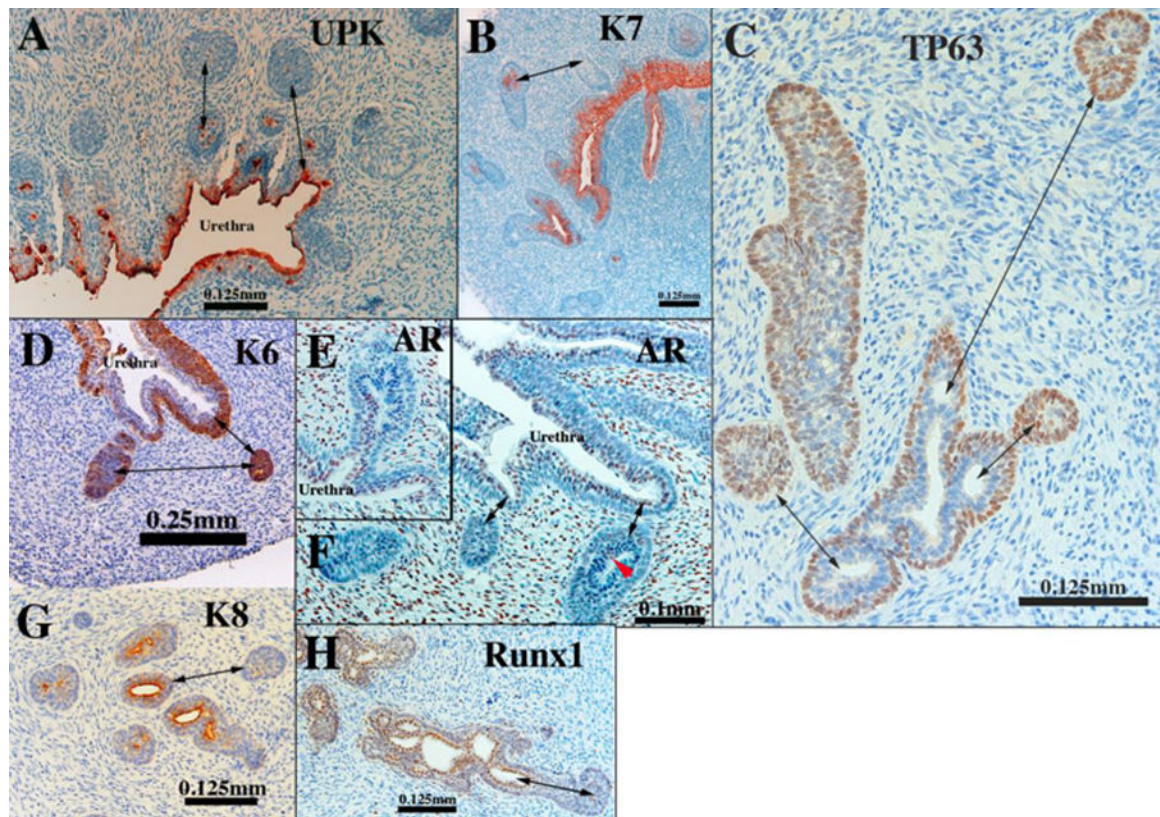
Figure 14.
Sections of human fetal prostatic ducts at or near the canalized-solid interface immunostained as indicated. In (E &F) note that AR is absent of solid epithelial cords, but present in canalized ducts. Double-headed arrows in emphasize differences between solid epithelial cords and canalized ducts.
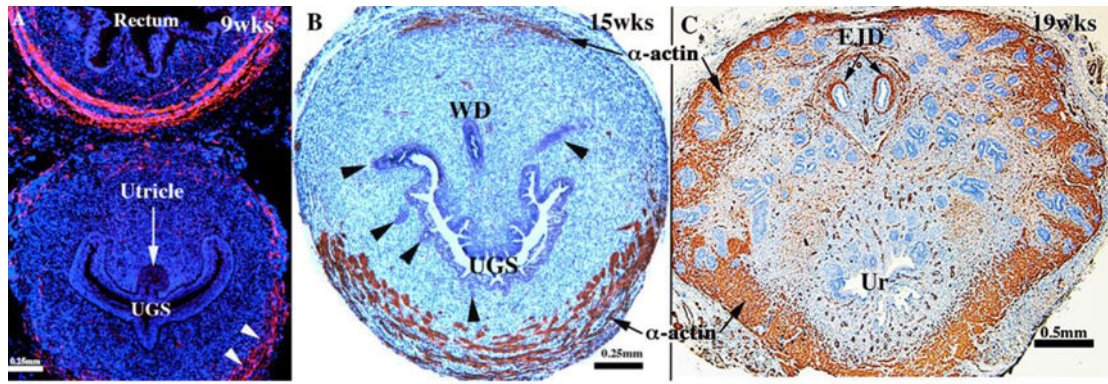
Figure 15.
Transverse sections of developing human prostate immunostained for smooth muscle α-actin. (A) is a section through the verumontanum of a 9-week pre-bud UGS in which sparse α-actin-positive cells (white arrowheads) are seen in ventral-lateral UGM, whereas α-actin-positive cells are abundant in the wall of the rectum. (B) is section of a human fetal prostate showing smooth muscle bundles in ventral UGM at 15 weeks of gestation. (C) is a section of a human fetal prostate at 19 weeks of gestation showing α-actin-positive smooth muscle around the periphery where solid epithelial cords are branching. WD= Wolffian duct, UGS= urogenital sinus, Ur= urethra, EJD=ejaculatory ducts.
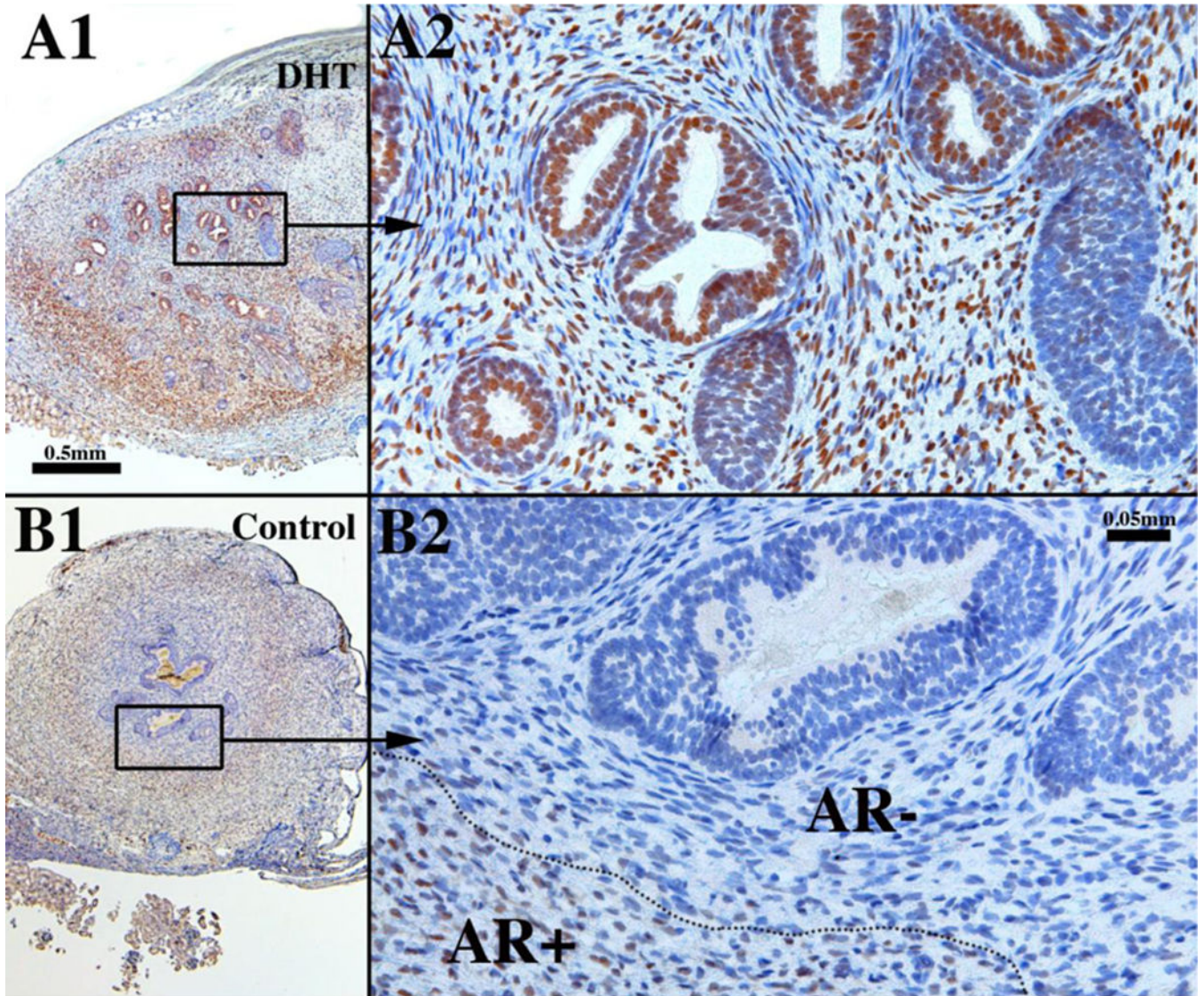
Figure 16.
Sections of xenografts of right and left halves of a 14-week human fetal prostate grown for 4 weeks in castrated male athymic mice treated with a 20mg pellet of dihydrotestosterone (DHT) (A1 & A2) or androgen-deficient control (sham) (B1 & B2) immunostained for androgen receptor. A small number of solid buds were present at the time of grafting. In the DHT-treated specimen, note the large number of ducts, many of which are canalized (A1 & A2), while in the androgen-deficient control specimen few ducts are seen and few are canalized (B1 & B2). Note the presence of AR broadly in epithelial and stromal cells in the DHT-treated specimen (A1 & A2). In the androgen-deficient control AR is absent (AR-) in the stromal cells in close association with the epithelium but is present in peripheral stroma (AR+) (B1 & B2).
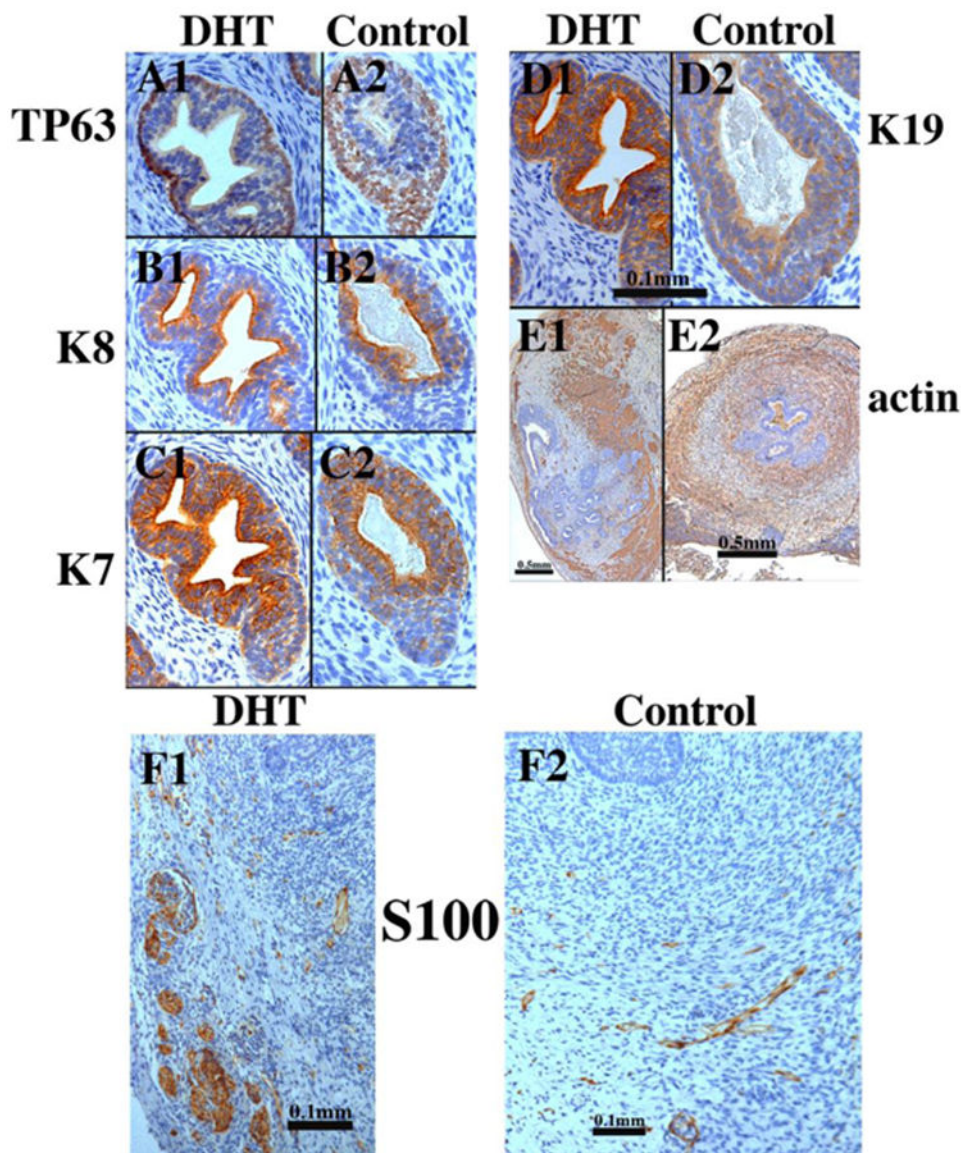
Figure 17.
Xenografts of right and left halves of a 14-week human fetal prostate grown for 4 weeks in castrated male athymic mice treated with a 20mg pellet of dihydrotestosterone (DHT) or untreated control (sham) as indicated. For TP63 and keratins 7, 8 and 19 the status of epithelial differentiation is advanced in DHT-treated specimens (Al-El)versus androgen-deficient control specimens (A2-E2). Patterning of α-actin-positive smooth muscle is also affected by DHT (El versus E2). S100-positive ganglia and nerve fibers were seen in both DHT-treated and control grafts (F1-F2). Scale bar in (D1 -D2) applies to (A-C).
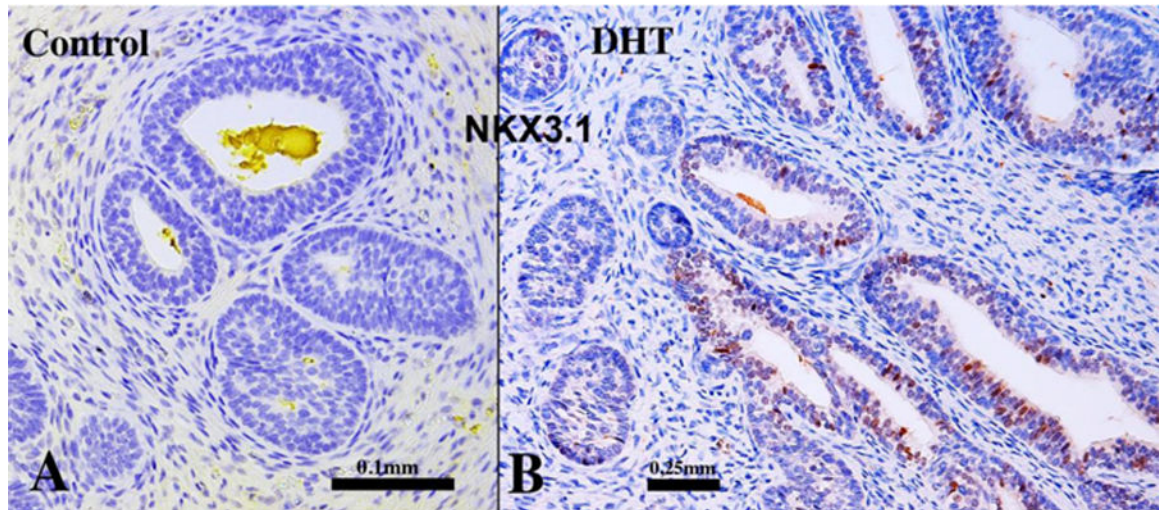
Figure 18.
Xenografts of right and left halves of a 14-week human fetal prostate grown for 4 weeks in castrated male athymic mice treated with a 20mg pellet of dihydrotestosterone (DHT) or untreated control (sham) as indicated immunostained for NKX3.1. Solid epithelial cords and canalized ducts observed in androgen-deficient control specimens were devoid of NKX3.1 immunostaining (A), whereas canalized ducts (but not solid epithelial cords) of DHT-treated specimens expressed NKX3.1 (B).
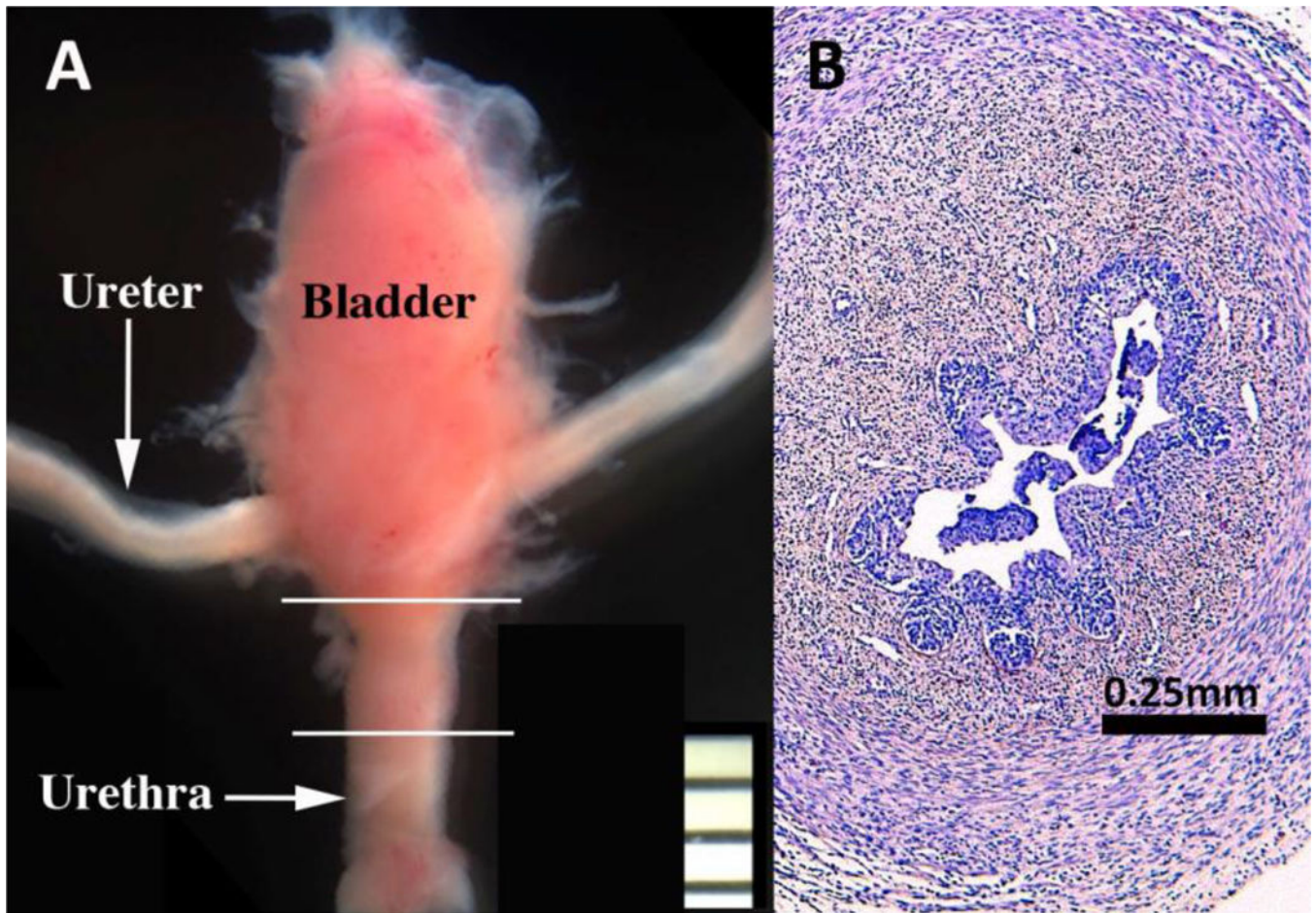
Figure. 19.
(A) Bladder, ureters and urethra of a 13-weeks human female fetus. White lines depict the segment of the female urethra that was xenografted into DHT- treated and untreated castrated mouse hosts. (B) Section of a 15-week human fetal bladder neck prior to grafting.

Figure 20.
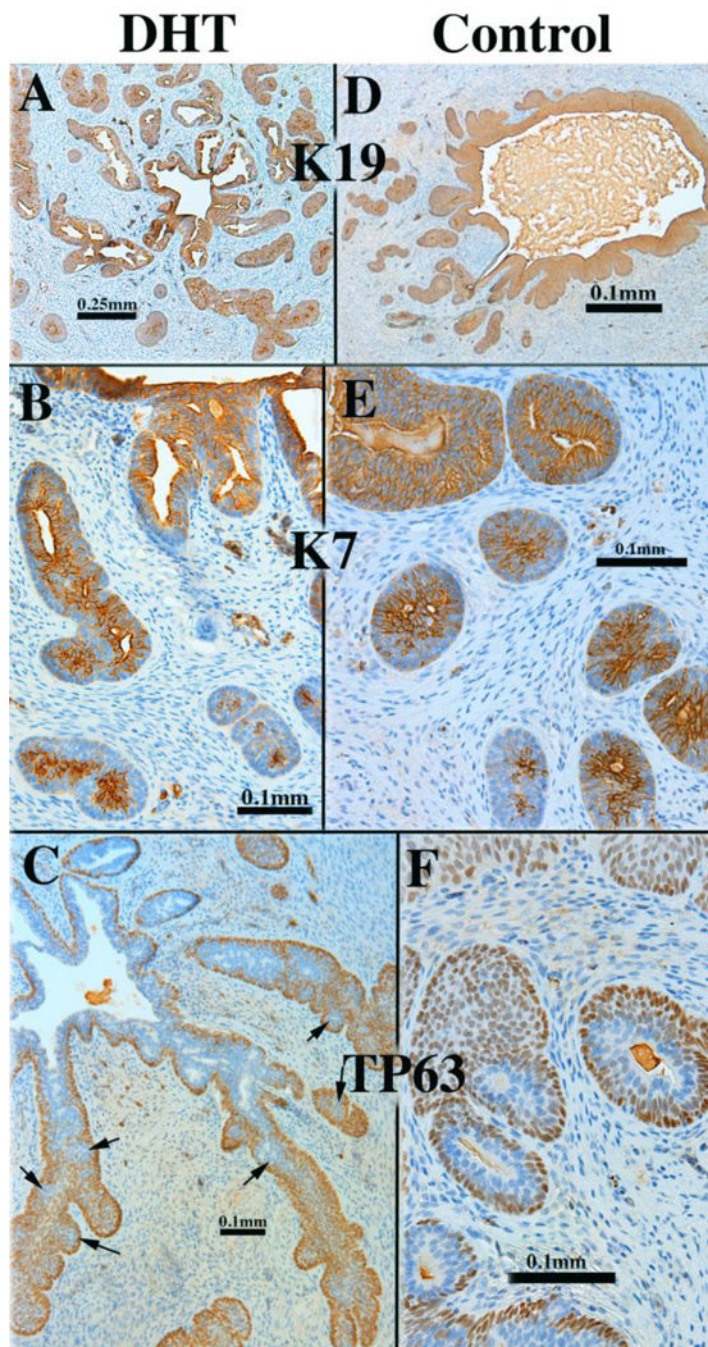Xenograft of a 12-week human fetal female urethra grown for 8 weeks in a castrated DHT-treated host (A-C) immunostained for KRT19, KRT7 and TP63 as indicated. Xenografts of a 13-week human fetal female urethra grown for 8 weeks in a castrated DHT-treated host (D-F) immunostained for KRT19, KRT7 and TP63 as indicated. Arrows in (C)) depict pockets of TP63-negative epithelial cells in areas of incipient canalization.
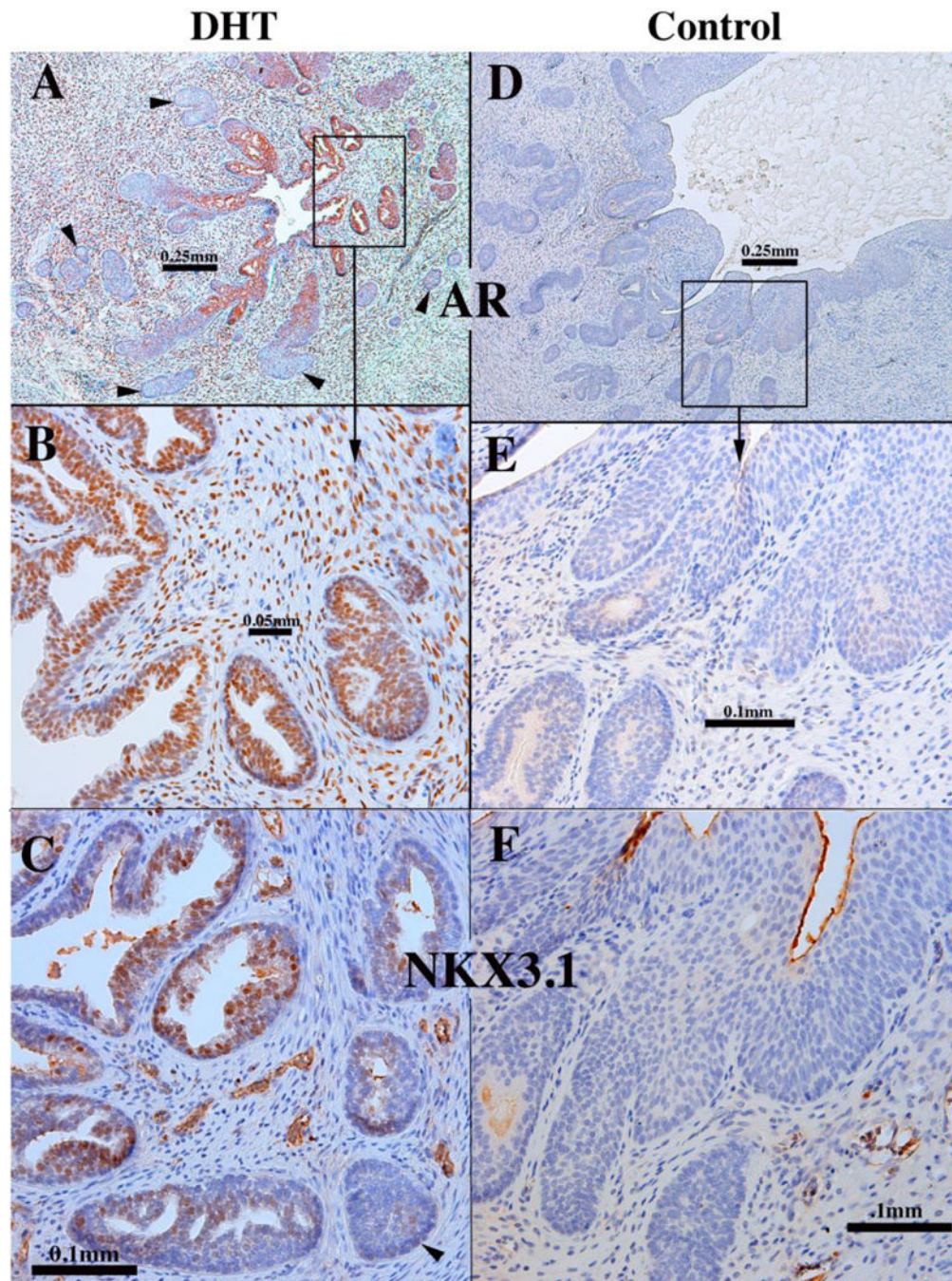
Figure 21.
A 12-week human fetal female urethra grown for 8 weeks in a castrated DHT-treated host (A-C). Xenograft of a 13-week human fetal female urethra grown for 8 weeks in an untreated castrated host (D-F). (A, B, D, E) were immunostained for androgen receptor (AR). (C & F) were immunostained for NKX3.1. Arrows in (A) and (C) highlight solid epithelial cords, which are mostly devoid of AR (A) and NKX3.1 (C).
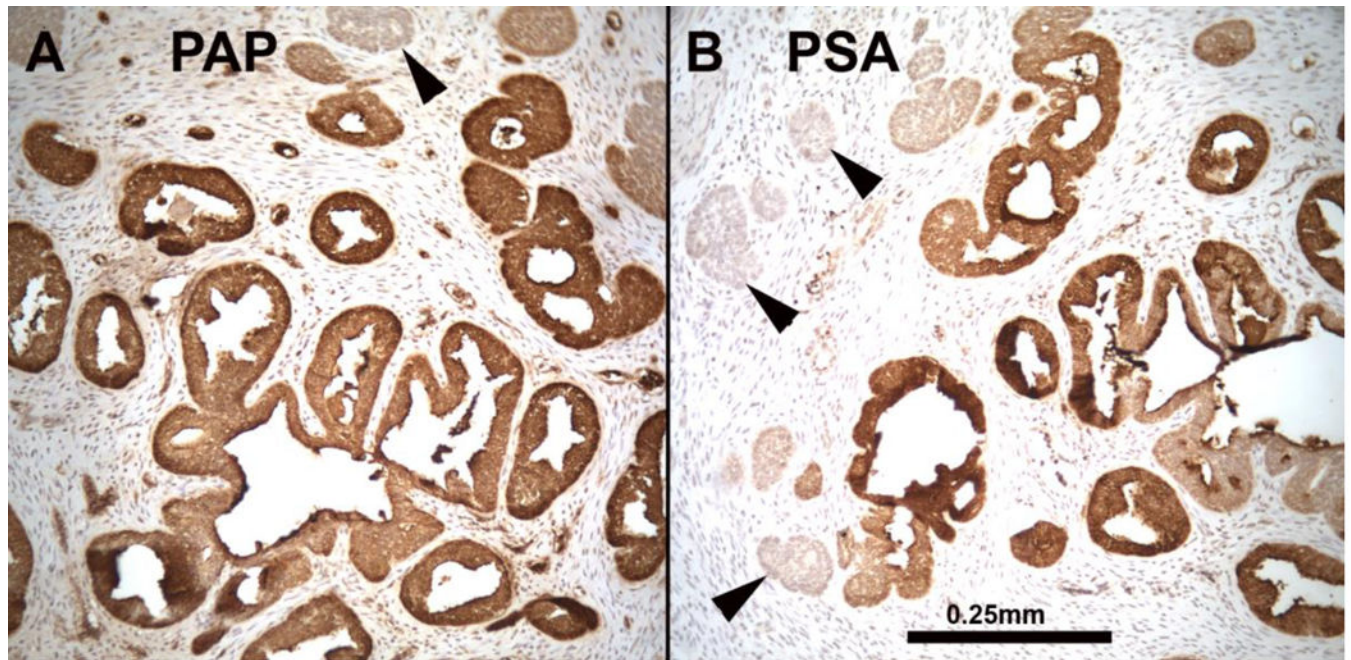
Figure 22.
A 12-week human fetal female urethra grown for 8 weeks in a castrated DHT-treated host immunostained for (A) prostatic acid phosphatase (PAP) and (B) prostatic specific antigen (PSA). PSA and PAP are expressed in ducts with lumina, but is reduced/absent in solid epithelial cords (arrowheads). Scale bar applies to both images.

Table 1.

Time line of human prostatic development in rats, mice and humans

Developmental event	Rat Age	Mouse age	Human Age	Human Crown-rump	Human Heal-toe
Pre-bud stage	14–18 dpc	13–15 dpc	8–9 wks	30–50mm	2–5mm
Initial budding	19 dpc	16–18 dpc	10–11 wks	50–60mm	5–8mm
Bud elongation & branching morphogenesis	1–50 dpn	1–40 dpn	11 wks & thereafter	70–80mm (11wks)	11mm (11wks)
Ductal canalization	~3–50 dpn	~3–50 dpn	11wks & thereafter	70–93mm (11–12wks)	12–14mm (11–12 wks)

dpc= days post-conception, dpn= days postnatal, wks=weeks

Table 2.

Published images of human prostatic bud elongation, ductal branching, ductal canalization and secretory cytodifferentiation.

Specimen Age (weeks)	Analysis/focus of paper	Reference
32, 38 & 40	Histology	(Zondek and Zondek, 1979)
28 & 30	Histology	(Xia et al., 1990)
22 & 28	Keratin IHC	(Wernert et al., 1987)
8–25	Neuroendocrine cell differentiation	(Xue et al., 2000; Szczyrba et al., 2017)
12, 16, 28, 29, 39	Sonic & desert hedgehog	(Zhu et al., 2007)
18, 19 & 23	Estrogen receptor beta (ESR2)	(Adams et al., 2002)
13 & 25	Striated & smooth muscle histochemistry	(Sebe et al., 2005)
19, 21 & 22	Estrogen receptor alpha & beta (ESR1 & 2)	(Shapiro et al., 2005a; Shapiro et al., 2005b)
19 to 36	Androgen receptor	(Aumuller et al., 1998)
9–16	Sonic hedgehog	(Barnett et al., 2002)
19–22	5a-reductase immunohistochemistry	(Radmayr et al., 2008; Levine et al., 1996; Lunacek et al., 2007; Bonkhoff et al., 1996)
18–23	SOX9 immunohistochemistry	(Wang et al., 2008)

Table 3

Epithelial differentiation markers reported previously in the developing human prostate

Markers	Pre-bud UGE	Solid buds	Canalized ducts Basal cells	Luminal cells	NE cells
KRT5/6,[1,6,12]		+	+	-	
KRT19[1,2,6,12]	+	+	+	+	
KRT18[1,6,12]	+	+	-	+	
KRT14[6,12]	+	+	+		
KRT8[6,12]	+	+		+	
TP63[1,6]	+	+	+	-	
AR[1,3,4,7,9]				+	
ESR[11,3,8]			-	-,+	
ESR2[3,8]		+	+	+	
PSA[1]		-	-	-	
EGFR[1]		+	+	+	
Bcl2[1]		+	+	+	
P27[1]		-	-	-	
5α-reductase[4,13,14]	Stroma= +				
SHH[5]		+		+	
DHH[5]		+		+	
PTC1 &PTC2[5]		+		+	
Glil[5]		+		+	
GSTpi[6]	+	+		+	
Chromogranin A[1011]					+
Serotonin[11]					+

(1) Letellier et al (2007)

(2) Wemert and Seitz (1987)

(3) Adams et al (2002)

(3) Levine et al 1996)

(4) Zhu et al (2007)

(5) Wang et al (2001)

(6) Saffarini et al (2013)

(7) Shapiro et al (2005)

(8) Aumuller et al (1998)

(9) Szczyrba et al (2017)

(10) Xue et al (2000)

(11) Trompetter et al (2008)

(12) Aumuller et al (1996)

(13) Radmayr et al (2008)

Table 4.

Antibodies used in this study

Antibody	Source	Catalogue #	Concentration
□ -actin	Sigma	A2547	1/2000
GTF3C2	Abcam	AB53218	1/100
Estrogen receptor □ (ESR1)	Abcam	Ab16660	1/100
Keratin 6	Acris Antibodies	AM21068PU-S	1/200
Keratin 7	E.B. Lane	LP1K	1/10
Keratin 8	E.B. Lane [*]	LE41	1/10
Keratin 10	Dako	M7002	1/50
Keratin 14	BioGenex	LL002	1/100
Keratin 15	Sigma	Sab4501658	1/50
Keratin 19	E.B. Lane [*]	LP2K	1/10
TP63	Santa Cruz Biotechnology	Sc-8343	1/100
Androgen receptor	Genetex	GTX62599	1/100
RUNX1	Abcam	Ab92336	1/100
Uroplakin1	T. T. Sun [**]		1/100
PAX2	Abcam	Ab150391	1/50
FOXA1	Atlas Antibodies	HPA050505	1/500
E-cadherin	BD Transduction Laboratories	610181	1/100
S100	Abcam	Ab52642	1/1000

[*] Institute of Medical Biology, Singapore

[**] New York University, New York

Table 5

Epithelial differentiation markers during human prostatic development

Markers	Pre-bud	Newly emerged solid buds	Bud elongation and branching		Canalized ducts (12–19wks)		
			Canalized	Solid	Basal cells	Luminal cells	Urethra
K6	+	+	+	+ & -	+	-	+
K7	+	+	+	- & - /+	-	+	+
K8	+	+	+	- &–/+	-	+	+
K10	-	-	-	-	-	-	-
K14	-	-	-	-	- & –/+	-	-
K15	-	+	+	+	+	-	+
K19	+	+	+	+	-	+	+
Runxl	?	+	+	+	- & –/+	+	+
P63	+	+	+	+	+	-	+
Foxa1	+	+	+	+	+	+	+
Pax2	-	-	-	-	-	-	-
Uroplakin	-	-	-	-	-	- & –/+	+
AR	+	+	+	+/–	- & –/+	+	+

Table 6.

Epithelial immunohistochemical profile of xenografts of human fetal prostates and human female urethras.

Markers[*]	Prostatic xenografts (DHT)	Female urethral xenografts (DHT)	Prostatic xenografts (control)	Female urethral xenografts (control)
Morphology	Canalized ducts	Canalized ducts	Solid "ducts"	Solid "ducts"
Keratin 7	Luminal cells only	Luminal cells only	Central cells[**]	Central cells[**]
Keratin 8	Luminal cells only	Luminal cells only	Central cells[**]	Central cells[**]
Keratin 14	Negative	Negative	Negative	Negative
Keratin 19	All epithelial cells	All epithelial cells	All epithelial cells	All epithelial cells
TP63	Basal cells only	Basal cells only	Basal & central cells	Basal & central cells
Androgen receptor	Luminal cells only	Luminal cells only	Negative	Negative
FOXA1	Positive	Positive	Positive	Positive
NKX3.1	Positive	Positive	Positive	Negative
PSA	ND	Positive	ND	Negative
PAP	ND	Positive	ND	Negative

[*] Only the predominant phenotype is reported. For additional information, see text.

[**] Central cells located in the core of solid ducts.

PSA=prostate specific antigen; PAP=prostatic acid phosphatase ND=not done